

Radiocarbon signatures of carbon phases exported by Swiss rivers in the Anthropocene

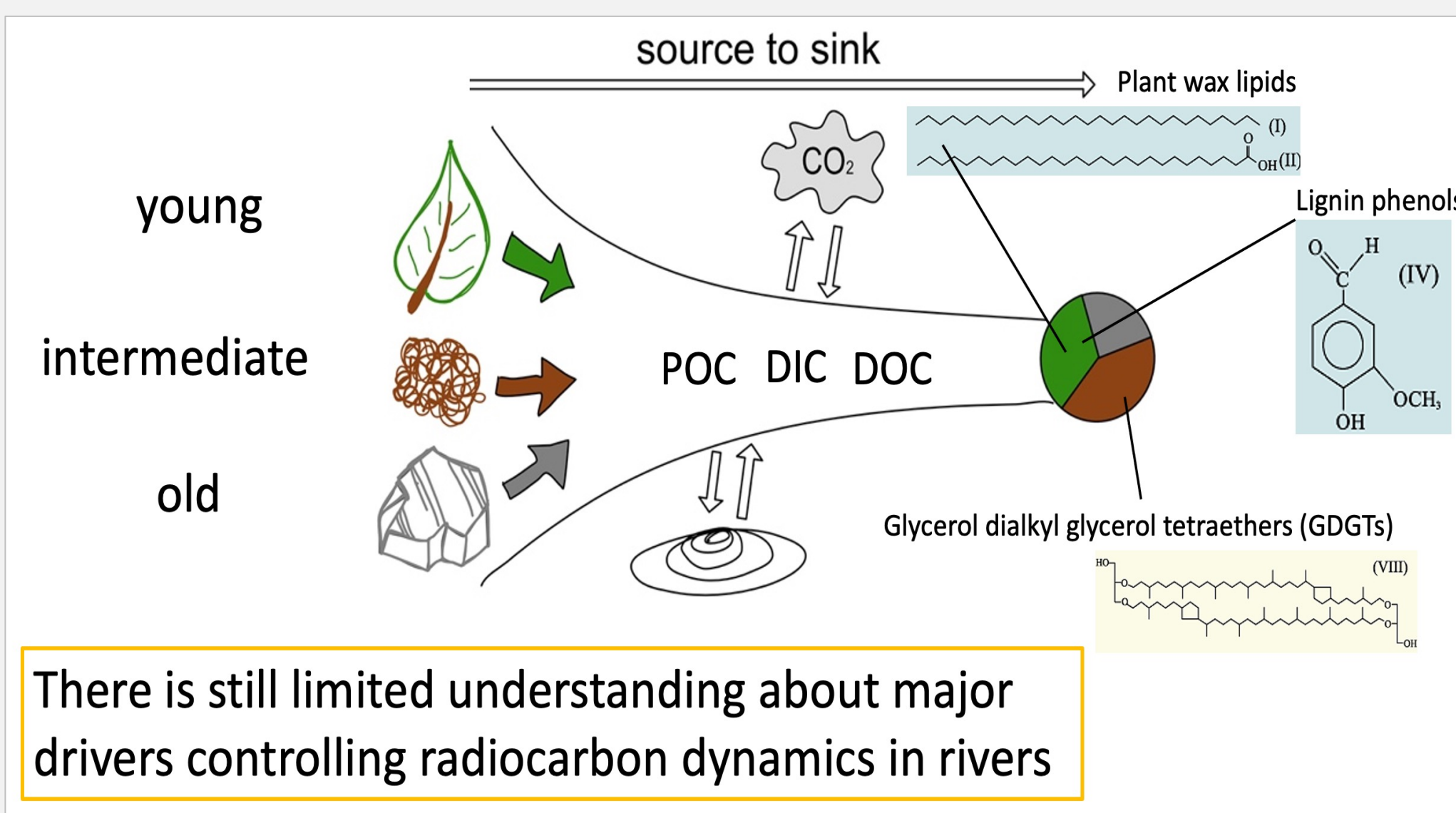
Timo M. Y. Rhyner^{a*}, Lisa Bröder^a, Margot White^a, Benedict V. A. Mittelbach^a, Alexander Brunmayr^e, Frank Hagedorn^d, Florian R. Storck^c, Lucas Passera^c, Negar Haghypour^{a,b}, Joerg Zobrist^f, and Timothy I. Eglinton^a

^a Geological Institute, ETH Zürich, 8092 Zürich, Switzerland, ^b Department of Physics, Laboratory of Ion Beam Physics, Zürich, Switzerland, ^c Hydrology Division, Federal Office for the Environment FOEN, Bern, Switzerland,

^d Swiss Federal Research Institute WSL, Birmensdorf, Switzerland, ^e Department of Physics, Imperial College London, London, UK, ^f Senior Eawag Emeritus, Herracherweg 103, Uster, Switzerland

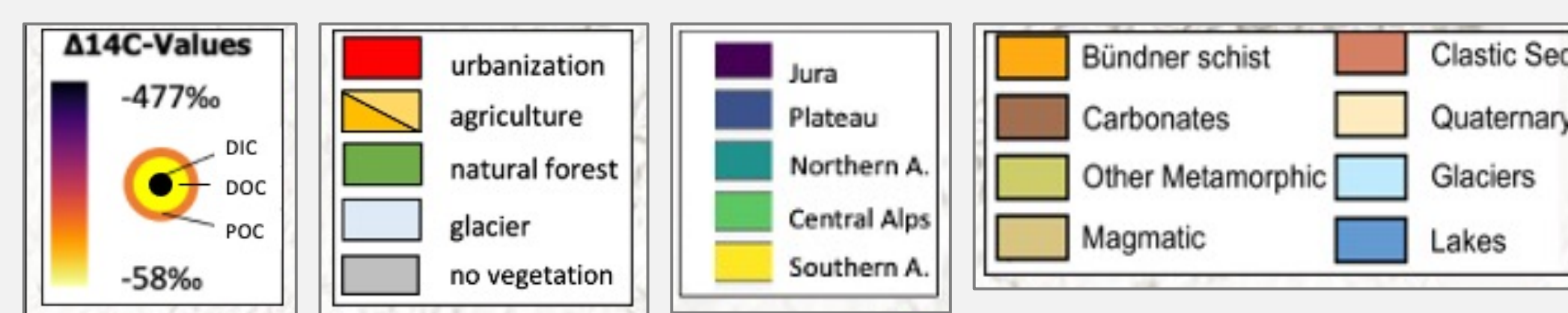
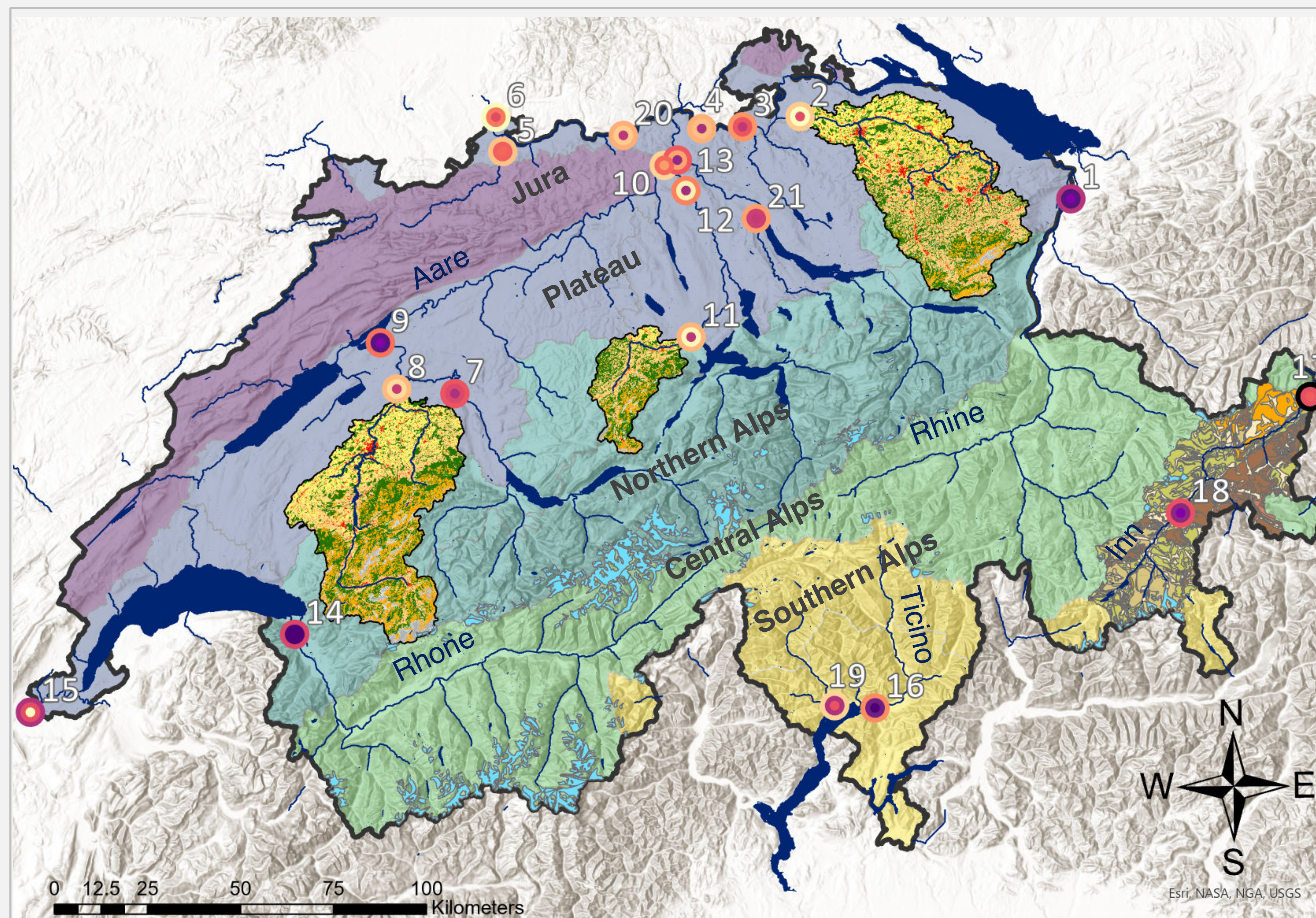
Why is this study important?

Rivers as sentinels of carbon dynamic change



Lateral carbon mobilization processes along the freshwater continuum are particularly prone to anthropogenic perturbations. Yet despite their importance as a key component of the C-cycle, they remain poorly constrained.

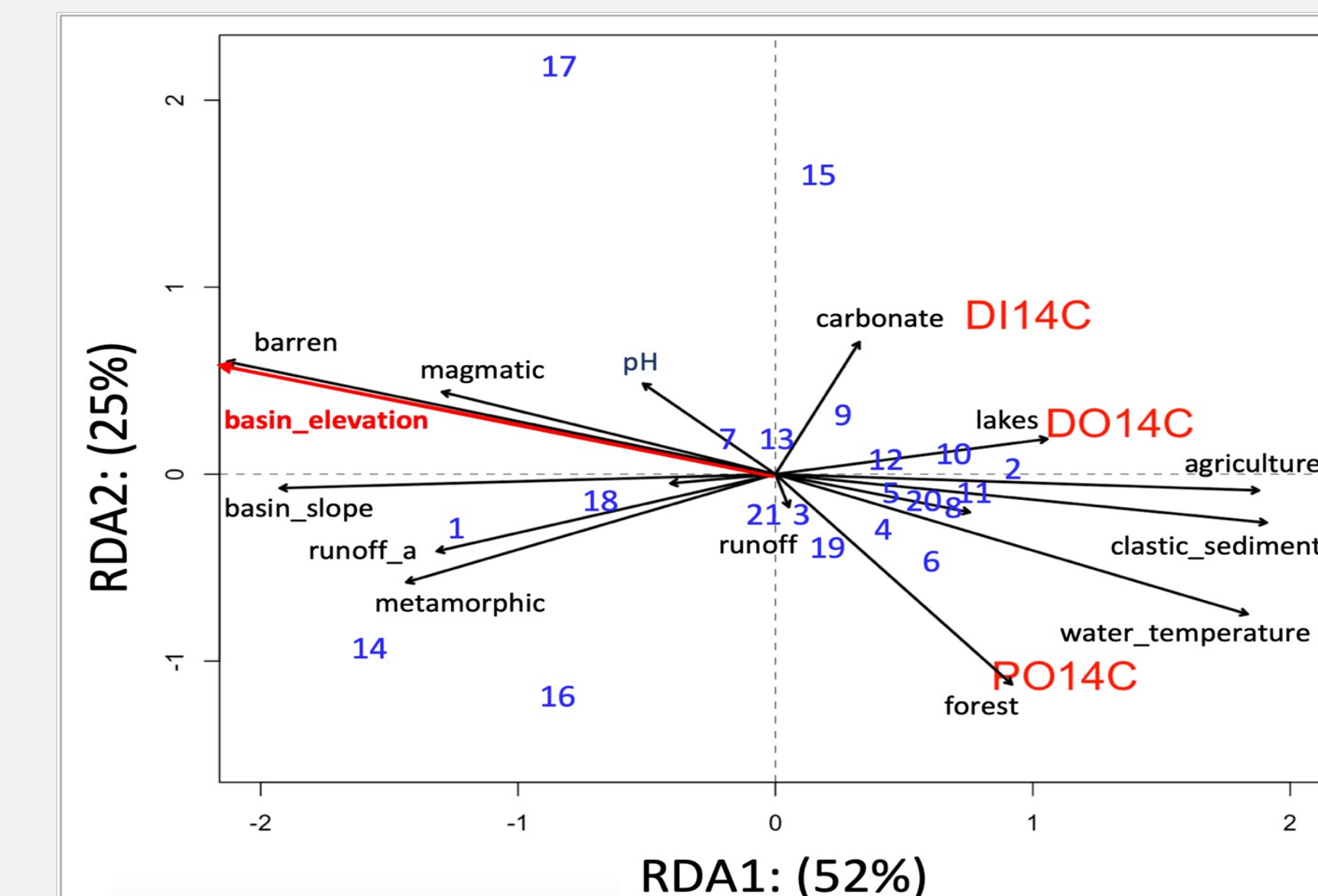
Where does the old/young carbon come from?



Samples have been obtained during high-flow conditions in summer 2021, a year of extraordinarily high rainfall. We examine a suite of 21 rivers draining the five different ecoregions of Switzerland (Jura, Plateau, Northern-, Central-, and Southern Alps), which are characterized by distinct climatic regimes, bedrock and vegetation types, and different levels of human pressure.

Results

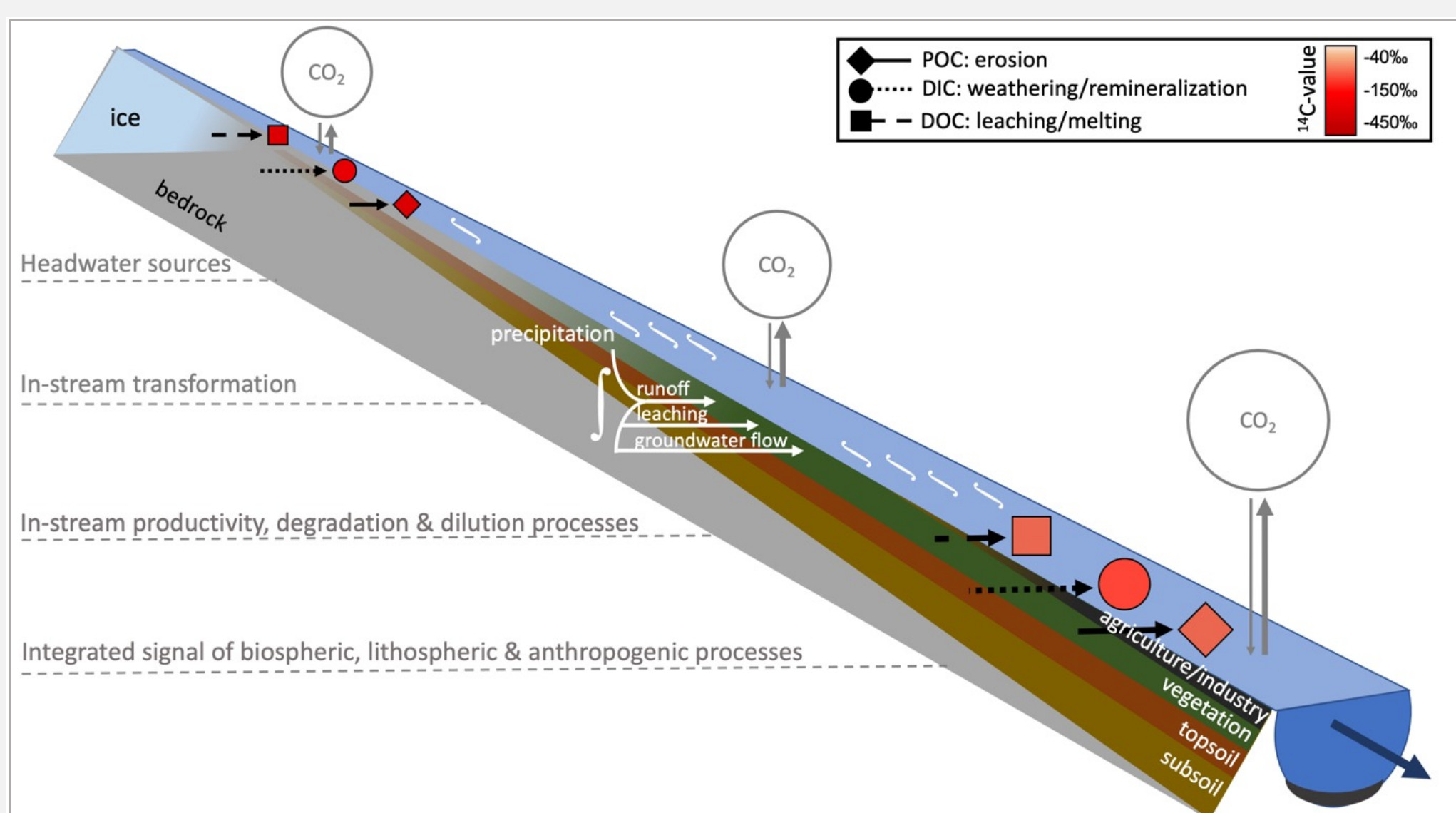
Basin elevation as the major control



Environmental variable loadings are in black arrows where significant vectors are illustrated in red (basin_elevation).

What is the main message?

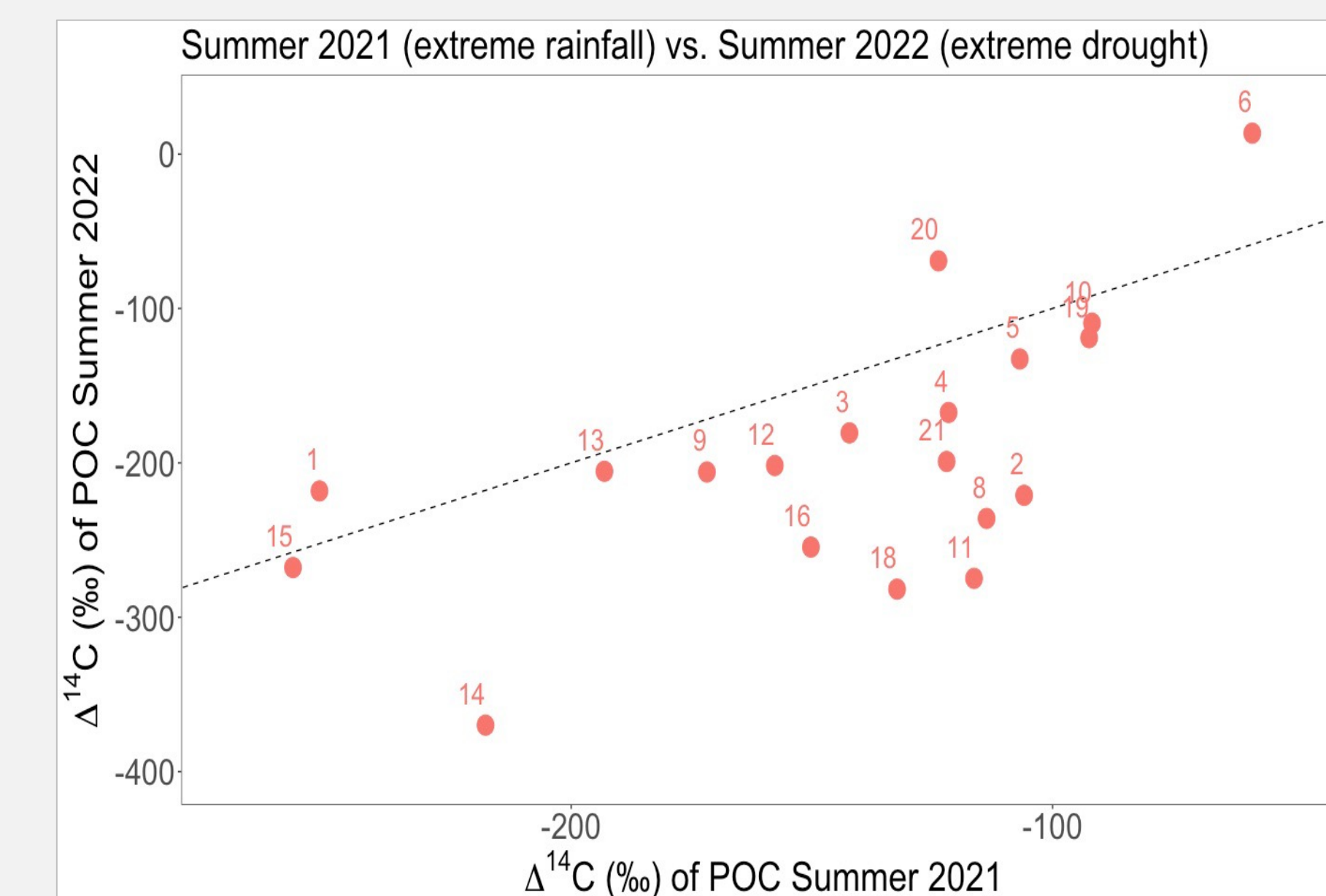
Radiocarbon ages become younger from Alps to Plateau



Conceptual figure summarizing the main findings of this study. These contrasts between alpine terrain and the lowlands reflect the importance of overriding (eco)regional controls on riverine carbon dynamics within Switzerland.

Future steps

Older POC during year of drought



¹³C-isotope measurements are needed to further constrain different source contributions.

PHILOSOPHICAL TRANSACTIONS OF THE ROYAL SOCIETY A

MATHEMATICAL, PHYSICAL AND ENGINEERING SCIENCES

Radiocarbon signatures of carbon phases exported by Swiss rivers in the Anthropocene

Journal:	<i>Philosophical Transactions A</i>
Manuscript ID	RSTA-2022-0326
Article Type:	Research
Date Submitted by the Author:	13-Feb-2023
Complete List of Authors:	Rhyner, Timo; ETH Zurich, Earth Science Bröder, Lisa; ETH Zurich, Earth Science White, Margot; ETH Zurich, Earth Science Mittelbach, Benedict; ETH Zurich, Earth Science Brunmayr, Alexander; Imperial College London, Department of Physics Haghipour, Negar; ETH Zurich, Ion Beam Physics Passera, Lucas; FOEN, Hydrology Division Storck, Florian R.; FOEN Hagedorn, Frank; Swiss Federal Institute for Forest Snow and Landscape Research WSL Zobrist, Jürg; Emeritus Scientist EAWAG Eglinton, Timothy; ETH Zurich, Earth Sciences
Issue Code (this should have already been entered and appear below the blue box, but please contact the Editorial Office if it is not present):	TM0522
Subject:	Biogeochemistry < EARTH SCIENCES, Environmental Chemistry (67) < CHEMISTRY (1002)
Keywords:	radiocarbon, Switzerland, rivers, carbon cycle, Anthropocene, climate change

SCHOLARONE™
Manuscripts

1
2
3 **Author-supplied statements**
4

5 Relevant information will appear here if provided.
6

7
8 **Ethics**
9

10 *Does your article include research that required ethical approval or permits?:*
11 This article does not present research with ethical considerations
12

13 *Statement (if applicable):*
14 CUST_IF_YES_ETHICS :No data available.
15

16
17 **Data**
18

19 *It is a condition of publication that data, code and materials supporting your paper are made publicly*
20 *available. Does your paper present new data?:*
21 Yes
22

23 *Statement (if applicable):*
24 All data is made available in tabular form in the manuscript and supplemental information.
25

26
27 **Conflict of interest**
28

29 I/We declare we have no competing interests
30

31 *Statement (if applicable):*
32 CUST_STATE_CONFLICT :No data available.
33
34
35
36
37
38
39
40
41
42
43
44
45
46
47
48
49
50
51
52
53
54
55
56
57
58
59
60

Radiocarbon signatures of carbon phases exported by Swiss rivers in the Anthropocene

Timo Rhyner^{a*}, Lisa Bröder^a, Margot White^a, Benedict V. A. Mittelbach^a, Alexander Brunmayr^e, Frank Hagedorn^d, Florian R. Storck^c, Lucas Passera^c, Negar Haghypour^{a,b}, Joerg Zobrist^f, and Timothy I. Eglinton^a

^a Geological Institute, ETH Zürich, 8092 Zürich, Switzerland

^b Department of Physics, Laboratory of Ion Beam Physics, Zürich, Switzerland

^c Hydrology Division, Federal Office for the Environment FOEN, Bern, Switzerland

^d Swiss Federal Research Institute WSL, Birmensdorf, Switzerland

^e Department of Physics, Imperial College London, London, UK

^f Senior Eawag Emeritus, Herracherweg 107, Uster, Switzerland

* Corresponding author: Timo Rhyner: timo.rhyner@erdw.ethz.ch

Abstract

Lateral carbon mobilization processes along the freshwater continuum are particularly prone to anthropogenic perturbations. Yet, they remain poorly constrained despite their importance as a key component of the C-cycle. This study examines the radiocarbon (¹⁴C) signatures of particulate and dissolved organic carbon (POC, DOC) and dissolved inorganic carbon (DIC) transported by Swiss rivers to assess their origin and controls on cycling of carbon within corresponding watersheds. Twenty-one rivers were selected and sampled during high-flow conditions in summer 2021, a year of extraordinarily high rainfall. Discharge (n=21) range from 7.4 m³/s to 2426 m³/s during sample collection. $\Delta^{14}\text{C}$ values of POC range from - 446‰ to - 158‰, while corresponding ranges of $\Delta^{14}\text{C}$ values for DOC and DIC are - 377‰ to - 43‰ and - 301‰ to - 40‰, respectively, indicating the dominance of pre-aged carbon. Based on Multivariate Regression Analysis, mean basin elevation correlated negatively with $\Delta^{14}\text{C}$ values of all three carbon phases. Rivers in the alpine terrain have lower $\Delta^{14}\text{C}$ values than rivers draining lower elevation terrain, where agricultural land-use is more intensive. These contrasts between alpine terrain and the lowlands reflect the importance of overriding (eco)regional controls on riverine carbon dynamics within Switzerland.

Keywords: Switzerland, radiocarbon, rivers, global carbon cycle, Anthropocene

Introduction

As the effects of anthropogenically-driven climate change are becoming a tangible reality, a deeper understanding about how these changes are linked to perturbations of Earth's carbon cycle is needed. Ongoing fossil CO₂ emissions since the era of industrialization together with substantial changes in land use are major contributors to climate change, where more frequent extreme weather events such as heatwaves, droughts and storms are superimposed on gradual changes in temperature and hydroclimate (Friedlingstein et al., 2022; Harris et al., 2018; Ripple et al., 2022; Trnka et al., 2014). Changes to the hydrological cycle affect the global carbon cycle where human activities alone have increased global erosion rates and transport of sediments to an extent which exceeds Earth's natural processes (Amundson et al., 2015; Gudmundsson et al., 2021.; Liu et al., 2021). Therefore, there is a need to constrain and quantify changes to the hydrological and carbon cycles at a broad range of scales, including regional to global, as well as to separate anthropogenic impacts from natural baselines (Friedlingstein et al., 2022; Galy et al., 2015; Regnier et al., 2022; Syvitski, 2003).

Lateral carbon fluxes represent important vectors that influence the fate of carbon taken up from the atmosphere by the terrestrial biosphere, transporting it from one reservoir to another and redistributing it along the land-to-ocean-aquatic-continuum (LOAC) (Regnier et al., 2022). These lateral processes are particularly prone to anthropogenic perturbations due to human activities of the land surface, yet remain poorly constrained (Battin et al., 2009; Regnier et al., 2013, 2022). In this regard, rivers serve as sentinels of carbon cycle change within their corresponding watersheds. They are natural integrators of processes occurring within their watersheds, mobilizing and transforming carbon during its movement from source to sink (Battin et al., 2009). Understanding of the role of rivers has evolved from the concept of a simple pipeline to a more reactive system interacting with its surroundings (Cole et al., 2007). In general, riverine carbon dynamics vary by catchment characteristics, such as geology, geomorphology, climate, and hydrology (Botter et al., 2019; Eglinton et al., 2021; Galy et al., 2015; Ran et al., 2018; Schwab et al., 2022; Voss et al., 2015). Extreme hydrologic events (e.g., heavy rainfall or snow/ice melting events) can have a large influence on carbon mobilization by shunting carbon from terrestrial interfaces to streams (Raymond et al., 2016). Human activities disrupt landscapes and the natural functioning of river systems, impacting in myriad ways including nutrient inputs from fertilizers, sewage discharge, and construction of dams for hydroelectric power and freshwater storage (Kelsey et al., 2020; Quéré et al., 2018; Raymond et al., 2008; Regnier et al., 2013; Tittel et al., 2022). However,

1
2
3 the relative importance of these different drivers, and their susceptibility to anthropogenic perturbation,
4
5 remains uncertain.

6
7 Radiocarbon (^{14}C) serves as a powerful tool to constrain carbon sources on a range of spatial
8
9 and temporal scales (Levin & Hesshaimer, 2000; Schuur et al., 2016; Szidat et al., 2006; Wacker et al.,
10
11 2013). Besides source apportionment, ^{14}C activity also enables the investigation of the controls on
12
13 ecosystem-scale carbon turnover times (Eglinton et al., 2021; Leifeld et al., 2009). Riverine carbon
14
15 sourced from vegetation, soil or bedrock (e.g., Ellis et al., 2012; Hemingway et al., 2017; Mccallister et
16
17 al., 2004; Raymond & Bauer, 2004; You et al., 2022) may exhibit sharply differing radiocarbon
18
19 characteristics, including modern biospheric carbon, pre-aged carbon stored in soils, and ancient
20
21 petrogenic carbon derived from rock weathering (Marwick et al., 2015). Radiocarbon ages of dissolved
22
23 organic carbon (DOC) tend to be relatively young, reflecting mostly fresh biospheric inputs (Catalán et
24
25 al., 2016; Galy et al., 2015; Marwick et al., 2015), whereas ^{14}C -ages for particulate organic carbon (POC)
26
27 generally range from old in the headwaters to young in the lowland rivers (Galy et al., 2015, 2015;
28
29 Marwick et al., 2015). The latter is possibly due to the dilution effects of old petrogenic carbon through
30
31 fresh inputs from vegetation litter (Schwab et al., 2022), or the result of remineralization processes
32
33 during fluvial transport (Galy et al., 2015; Marwick et al., 2015). The radiocarbon characteristics of
34
35 riverine dissolved inorganic carbon (DIC) are related to gas exchange with the atmosphere, organic
36
37 matter remineralization processes and bedrock chemical weathering pathways. With respect to the
38
39 latter, riverine DIC can either exhibit modern ^{14}C -ages, representing silicate weathering by carbonic acid
40
41 derived from precipitation, intermediate ages stemming from carbonic acid weathering of carbonate
42
43 rocks, or fossil ^{14}C -signatures reflecting weathering of carbonates by sulfuric acid or oxidation of
44
45 petrogenic OC (Blattmann et al., 2019; Galy et al., 2015; Marwick et al., 2015). Consequently, riverine
46
47 DIC tends to be generally older in mountainous headwaters. Depending on the weathering regime it can
48
49 represent either a source or a sink for atmospheric CO_2 and reflect a significant carbon input to upland
50
51 streams (Gaillardet et al., 2019; Horan et al., 2019).

52
53 Prior ^{14}C studies in rivers have mainly focussed on major river systems due to their global
54
55 importance in regulating freshwater and materials fluxes to the ocean (Aufdenkampe et al., 2011;
56
57 Marwick et al., 2015). More recent work has highlighted the collective role of small, mountainous river
58
59 systems draining active continental margins (e.g., Taiwan) as globally important vectors for sediment
60
and carbon translocation and export (Hilton et al., 2011; Kao et al., 2014). Other studies have
emphasized the importance of smaller headwater streams and inland waters along the LOAC as

1
2
3 components of the global carbon cycle (Regnier et al., 2022; Xenopoulos et al., 2017). While many prior
4 studies tend to focus on either the inorganic or organic phase of carbon due to contrasting (e.g.,
5 geochemical or ecological) approaches (Galy et al., 2015; Gies et al., 2022; Hilton et al., 2011; Keil et
6 al., 1997; Raymond et al., 2004; Voss et al., 2015), relatively few studies examine all three C phases
7 (DIC, DOC, POC), especially from a ^{14}C perspective (Kelsey et al., 2020). However, given the intimate
8 relationships between these different phases and the potential for carbon exchange between them
9 simultaneous characterization of all 3 carbon phases is desirable, and provides a window into the
10 interplay of carbon dynamics within the freshwater aquatic continuum (Regnier et al., 2022).

11
12
13
14
15
16
17
18
19
20
21
22
23
24
25
26
27
28
29
30
31
32
33
34
35
36
37
38
39
40
41
42
43
44
45
46
47
48
49
50
51
52
53
54
55
56
57
58
59
60
Switzerland, particularly its alpine regions, is experiencing environmental and ecosystem
change at a more rapid pace than most regions of the world (Bolliger et al., 2008; Zubler et al., 2014).
Rapidly retreating glaciers, decreasing snow coverage, alpine greening, and increasing intensity and
frequency of extreme rain events and droughts are manifestations of this change (Bolliger et al., 2008;
Hagedorn et al., 2008; Leifeld et al., 2005, 2009; Zubler et al., 2014). Over the past 4 decades, river
water temperatures increased by 0.8-1.3 °C, while water discharge remained largely unchanged. For
the major three rivers in Switzerland (Rhine, Rhone, and Ticino) there was a small but statistically
significant increase in DIC concentrations over the past 4 decades (Zobrist et al., 2018). This suggests
increased DIC inputs from bedrock weathering, belowground respiration or soil OM remineralization in
aquatic systems all of which are potentially accelerated by increasing temperatures due to climate
change.

These observations provide motivation for the present study, which investigates the ^{14}C -isotopic
characteristics of POC, DOC, and DIC currently transported by and exported from Swiss rivers. We
examine a suite of 21 rivers draining the five different ecoregions of Switzerland (Jura, Plateau,
Northern-, Central-, and Southern Alps), which are characterized by distinct climatic regimes, bedrock
and vegetation types, and different levels of human pressure (Botter et al., 2019; Nussbaum et al.,
2014). Because the different major drainage basins of Switzerland map onto these ecoregions, they
lend themselves to the assessment of regional-scale controls on the amount and composition of carbon
exported by the different river systems and provide a window into the impact of future scenarios of
climate change on Swiss landscapes. In order to isolate major drivers, we conduct a Multivariate
Regression Analysis, incorporating in-situ water quality measurements and the long-term NADUF
hydrological dataset (National Long-Term Surveillance of Rivers) combined with catchment
characteristics, land-use, and lithology. Ultimately, we seek to develop a predictive capability based on

radiocarbon signatures for assessing the sources and pathways of carbon within the aquatic continuum as a function of differences in catchment characteristics that may inform on future changes of the C-cycle in response to direct and indirect anthropogenic perturbation.

Methods

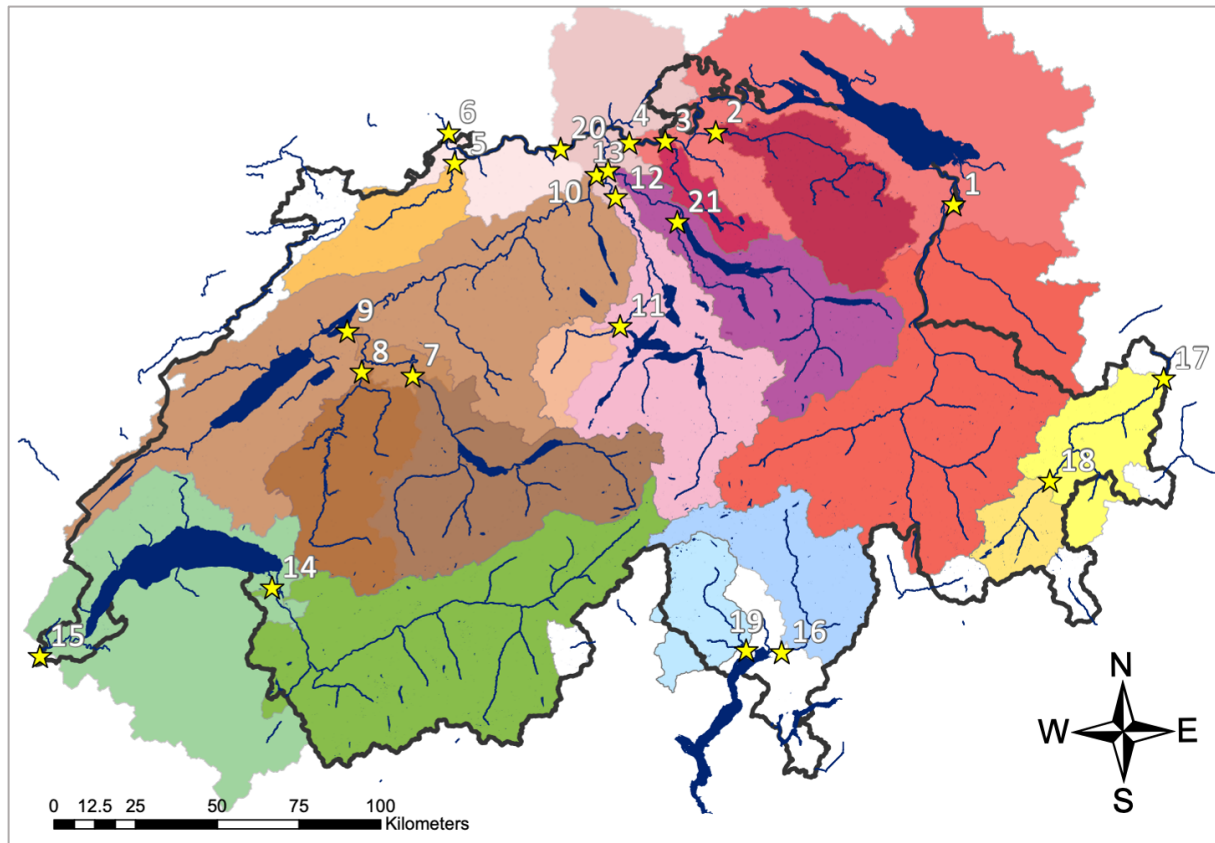


Figure 1: Map of Switzerland with 21 river sampling stations indicated as numbered stars. Watershed areas of corresponding stations are illustrated in different colors. In blue, lakes and water ways of major rivers are indicated where the four major rivers are labeled accordingly. The Swiss boarder is indicated as a dark grey line.

a. Study Site and Sampling Stations

Switzerland hosts a plethora of river systems, including the headwaters of the four major central European rivers – the Rhine, Rhone, Ticino (Po), and Inn (the latter two representing headwaters of the Po and Danube, respectively). Lakes Constance, Geneva and Maggiore are the intermediate receiving basins for the Upper Rhine, Upper Rhone and Ticino rivers, respectively. Rivers in Switzerland are exceptionally well monitored regarding their discharge and water chemistry, primarily as a result of the NADUF program (National Long-Term Surveillance of Rivers), which has been reporting on-going changes in Swiss rivers and their watersheds for 50 years (Botter et al., 2019; Storck et al, 2022; Rodríguez-Murillo et al., 2015; Zobrist et al., 2004, 2018; Zobrist & Reichert, 2006). A total of 21

1
2
3 sampling stations on these and other Swiss rivers were chosen to align with those of the NADUF
4 program (Figure 1). In addition to the NADUF-stations, two additional rivers - the Sihl River (Brunau,
5 station 21) which represents a smaller tributary of the Limmat catchment and the Maggia River (Locarno,
6 station 19) were chosen, the former (and its headwaters) being the focus of prior in-depth investigations
7 (Gies et al., 2022; Schwab et al., 2022).
8
9
10
11

12 Land-use within the different river basins differs considerably. The northern part of Switzerland,
13 the Swiss Plateau, is heavily anthropogenically impacted and is primarily characterized by agricultural
14 land use (cropland) and urban settlements. In contrast, while also anthropogenically perturbed, alpine
15 regions are covered by natural and managed forests, pastures, and mostly unproductive areas due to
16 steep terrain and barren land surfaces (Bolliger et al., 2008) (SI: Table 1). Pressures related to
17 agricultural land-use follow a general gradient of increasing anthropogenic perturbation from south to
18 north, although extensive practices of agriculture are common in the southern part of Switzerland
19 (canton Ticino) and patches of urbanization are also found in some mountainous valleys.
20
21
22
23
24
25
26
27

28 Underlying bedrock can be an important factor influencing the age and amount of both POC and DIC
29 found in rivers. Switzerland is covered by a variety of lithologies, which for this study are categorized
30 into five groups (SI: Table 1). Magmatic rocks are commonly found in the central Alps, where the
31 headwaters of most major Swiss rivers are located. Metamorphic rocks like gneiss and schists are
32 commonly found in the south and east of Switzerland. Carbonate rocks, like limestone and dolomite,
33 form large parts of the pre-Alps and the Jura mountains in the north of the country. DIC is especially
34 affected by the chemical weathering of carbonate rocks, where they contribute old, i.e., radiocarbon-
35 dead, carbon to the DIC pool (Blattmann et al., 2019; Raymo & Ruddiman, 1992). Sedimentary rocks,
36 such as slates and shales, mostly of marine origin, are found in the uppermost Rhine valley and the
37 Engadin. Riverine POC can be affected by the erosion of petrogenic OC from such sedimentary rocks,
38 which contain ancient OC (kerogen). Siliciclastic sediments and unconsolidated quaternary sediments
39 are found in the Swiss Plateau region, where the latter is also found along the major river valleys in all
40 regions (Vandenbroucke & Largeau, 2007).
41
42
43
44
45
46
47
48
49
50
51
52

53 Streamflow seasonality in Swiss river systems is foremost governed by precipitation and
54 snowmelt (Rodríguez-Murillo et al., 2015; Zobrist et al., 2018; Zobrist & Reichert, 2006). Additionally,
55 hydropower facilities also significantly influence the discharge of Swiss rivers. Generally, the maximum
56 discharge occurs during the spring season, with alpine rivers exhibiting stronger seasonality due to snow
57 and ice melt and are characterized by high discharge not only during the spring but also during the
58
59
60

1
2
3 summer season (Botter et al., 2019; Zobrist et al., 2018). Compared to a rapid response in peak flow for
4 alpine rivers, monitoring stations located downstream of major lakes respond rather slowly and modestly
5 to flood events (Botter et al., 2019; Rodríguez-Murillo et al., 2015; Zobrist et al., 2018).
6
7
8
9

10 *b. Sampling Methodology*

11
12 River waters were sampled between the 8th of May and 25th of August 2021. For this study, we
13 focus on periods of high discharge events since previous studies have shown that most of the carbon
14 in rivers is transported during high flow conditions (Botter et al., 2019; Gies et al., 2022; Zobrist et al.,
15 2018). We therefore only report data corresponding to the sampling date with the highest discharge on
16 the premise that this represents the dominant radiocarbon signatures for each river (SI: Table 2).
17 Surface water samples (< 0.5 m) were collected from the middle of the river channel (usually from
18 bridges) using a pre-rinsed metal bucket. Using a custom-made filtration system, the river water was
19 filtered through a 90 mm diameter and 0.2 µm pore size polyether sulfone (PES) filter using a bicycle
20 pump for pressurization (max. press., 2 bar) (Galy et al., 2011; Hilton et al., 2011). For POC
21 determination, these PES filters were placed into 40ml pre-combusted glass vials or aluminum foil
22 pouches and then stored in the freezer (-20 °C) prior to analysis. Before sample preparation, PES-filters
23 were freeze dried and then wetted with MilliQ-water, then the vials were placed into the ultrasonic bath
24 and vortexed to efficiently remove the sediments from the filters. Sediment suspensions were then
25 freeze dried before subsampling. Only for one station (station 12 at Mellingen), pre-combusted glass
26 fibre (GFF) filter of 0.7 µm pore size has been chosen, using a pre-combusted glass filtration set-up and
27 a vacuum-pump. After freeze drying the GFF-filter, several 4mm circles were punched out and placed
28 into silver boats before fumigation. DOC samples (filtrate) were collected in pre-combusted amber glass
29 bottles (250 ml) and stored in the freezer at -20 °C until measurement. DIC was sampled separately
30 using a 50 ml syringe and 0.2 µm PES Sterivex-filter to remove particulate matter. The filtrate was
31 sampled into 12ml exetainer vials pre-poisoned with mercuric chloride (HgCl₂) to avoid bacterial activity
32 and subsequently stored cold (4 °C) in the dark prior to measurement.
33
34
35
36
37
38
39
40
41
42
43
44
45
46
47
48
49
50
51
52
53
54

55 *c. Analytical Methods*

56 Radiocarbon analyses were conducted using a MICADAS (Mini Carbon Dating System) Accelerator
57 Mass spectrometer (AMS) (Synal et al., 2007) equipped with a Gas Interfaces System (GIS) and CO₂-
58 accepting ion source at the Laboratory for Ion Beam Physics (LIP) in the Department of Physics at the
59
60

1
2
3 ETH Zurich. Before being wrapped into tin capsules, approximately 25 mg of suspended matter (POC)
4 was weighed into silver capsules and then fumigated over HCl (37%) vapors (65°C, 72h) to remove
5 inorganic carbon and subsequently neutralized by exposure to sodium hydroxide pellets (65°C, 72h).
6
7 Collection year must be specified in order for $\Delta^{14}\text{C}$ results to be calculated. ^{14}C is reported as $F^{14}\text{C}$ and
8 measured using the on-line elemental analyzer (EA)-AMS system (McIntyre et al., 2017). For DO^{14}C ,
9 around 30ml of pre-filtered water was freeze dried. Then phosphoric acid (85%) was added to remove
10 DIC. A wet chemical oxidation (WCO) method is applied, which is based on using aqueous persulfate
11 oxidant to oxidize the water sample, and subsequent purging and radiocarbon analysis of released CO_2
12 through an automated headspace sampler coupled to the MICADAS (Lang et al., 2016). All the DOC
13 samples have been corrected with the constant contamination ($M_c=0.98 \pm 0.45$, $F^{14}\text{C}=0.39 \pm 0.08$)
14 method according to Hanke et al., 2017. DI^{14}C -samples have been purged with helium in order to release
15 atmospheric CO_2 from the DIC-sample. Then 250 μl of phosphoric acid (85%) is added into the samples.
16 This CO_2 in the headspace which was converted from DIC of the vial was introduced to the gas interface
17 system (GIS) (Fahrni et al., 2010) and measured with the gas ion source of MICADAS. For all the DIC
18 samples, C1 (IAEA) was used as a blank material and C2 (IAEA) was used as a secondary reference
19 material. All ^{14}C -values are reported as $F^{14}\text{C}$ -values according to (Stuiver & Polach, 1977) which are
20 then converted to $\Delta^{14}\text{C}$ -values ($\Delta^{14}\text{C} = [F_m * e^{\lambda(1950-Y_c)} - 1] * 1000$), where λ is the inverse of the true
21 mean-life of radiocarbon and Y_c is the year of collection. The $\Delta^{14}\text{C}$ is age corrected to account for decay
22 that took place between collection (or death) and the time of measurement so that two measurements
23 of the same sample made years apart will produce the same calculated $\Delta^{14}\text{C}$ result.
24
25
26
27
28
29
30
31
32
33
34
35
36
37
38
39
40
41
42
43

44 *d. Statistical Analysis*

45
46 In order to examine potential relationships between response and control variables an ordinary
47 least square (OLS) Multivariate Regression Analysis (MRA) analysis was performed according to
48 standardized procedures (Draper, 2002) and plotted as a Redundancy Analysis (RDA). We standardized
49 all values in order to facilitate comparisons between various parameters of different units. All statistical
50 analysis were conducted using R-studio version 13 (Eddelbeuttel and Francois, 2011) with the vegan
51 package (Oksanen et al., 2020). The snapshot dataset of bulk $F^{14}\text{C}$ -values for all three carbon phases
52 (POC, DOC, and DIC) corresponding three carbon phases are selected as response variables, whereas
53 different watershed parameters - land cover, lithology, topography - and climatic, hydrologic as well as
54 anthropogenic variables were selected as the control. A digital elevation map (DEM) is calculated for
55
56
57
58
59
60

1
2
3 the relief analysis (calculation of the partial catchment areas and flow paths) using the software ArcGIS
4 version 10 (ESRI 2011). The methodology is based on the use of official governmental digital data,
5 where the control variables about land cover were calculated as the basin average according to the
6
7 “Areal Coverage Data Set 2020”, provided by Federal Office for the Environment (FOEN; URL in
8
9 References). For lithology coverage “Origin of Rocks 500 Data Set” was used (provided by FOEN; URL
10
11 in References). All other control variables such as information about catchment topography, climate, and
12
13 hydrology was compiled from the data set of the National Long-Term Surveillance of River Program
14
15 (NADUF; URL in References).
16
17
18
19

20 **Results**

21 *a. River Discharge and Water Chemistry*

22
23
24 The sampling was conducted during summer 2021, which subsequently emerged as a year of
25
26 extreme rain events. This resulted in exceptionally high discharge in Swiss rivers that had not been
27
28 witnessed in decades. For example, at station 6 (Weil) - the most downstream station of the Rhine with
29
30 a watershed area covering the majority of the Swiss territory, average discharge measured by the
31
32 NADUF-Program during 2021 was 2719 m³/s. This value of discharge has not been exceeded since the
33
34 summer of 1999 (3217 m³/s) (NADUF). For most of the sampling stations, it was possible to capture the
35
36 peak of discharge during the year of 2021 (SI: Table 2), and thus our snapshot samples primarily reflect
37
38 high discharge events.

39
40 The last station of the Rhine River (station 6 at Weil and 20 at Laufenburg) exhibited the highest
41
42 discharge at the time of sampling of 2426 and 2400 m³/s, respectively, followed by station 10 (Brugg) of
43
44 the Aare River and station 1 (Diepoldsau) of the Rhine River with 737 m³/s and 466 m³/s, respectively
45
46 (Table 1). The Glatt River (station 3 at Rheinsfelden), in contrast, showed the lowest discharge of 7.4
47
48 m³/s during our sampling in 2021. Average river water temperature of our sampling set was 16.4 ± 3.8
49
50 °C (n=21). The maximum temperature value (22.5 °C) was at station 3 (Glatt River at Rheinsfelden),
51
52 whereas the minimum (9.2 °C) was at station 17 (Inn River at Martina). Average river water pH value of
53
54 our sampling set was 8.3 ± 0.14. The maximum pH value was at station 17 (Inn River at Martina) with a
55
56 value of 8.5, whereas the minimum was a pH of 7.9 at station 19 (Locarno) on the Maggia River (SI:
57
58 Table 3).
59
60

Table 1: Table about study site information, mean basin area, mean basin elevation, average monthly discharge of all available data for the same sampling month, sampling date, and corresponding discharge. The last column shows the factor of discharge during sampling compared to monthly average of all FOEN data of the same month.

Station	Name	Area (km ²)	Elevation (m)	Monthly Discharge (m ³ /s)	Date	Discharge (m ³ /s)	factor
1	Rhein-Diepoldsau	6119	1771	448 (1983-2018)	25.06.21	466	1.0
2	Thur-Andelfingen	1696	773	49.9 (1904-2018)	19.07.21	129	2.6
3	Glatt-Rheinsfelden	417	506	8.75 (1976-2018)	28.06.21	7.4	0.8
4	Rhein-Rekingen	14767	1134	670 (1904-2018)	28.06.21	614.3	0.9
5	Birs-Münchenstein	14718	733	11 (1917-2018)	22.07.21	29.5	2.7
6	Rhein-Basel	36472	1055	1457 (1891-2018)	22.07.21	2426	1.7
7	Aare-BernSchönau	2941	1591	211 (1935-2018)	07.07.21	331	1.6
8	Sanne-Gümmenen	1881	1135	15.2 (1981-2018)	07.07.21	107.5	7.1
9	Aare-Hagneck	5104	1368	263 (1984-2015)	07.07.21	435	1.7
10	Aare-Brugg	11726	1003	376 (1935-2018)	09.08.21	737	2.0
11	Kleine Emme-Littau	478.3	1058	11.3 (1985-2018)	12.07.21	21.1	1.9
12	Reuss-Mellingen	3385	1258	191 (1935-2018)	02.08.21	385.7	2.0
13	Limmat-Gebenstorf	2393	1066	114 (1951-2018)	09.08.21	179	1.6
14	Rhône-Porte du Scex	5244	2124	351 (1935-2018)	06.07.21	285	0.8
15	Rhône-Chancy	10323	1570	512 (1935-2018)	06.07.21	430	0.8
16	Ticino-Riazzino	1613	1643	148 (1999-2005)	20.05.21	77.8	0.5
17	Inn-Martina	1941	2342	71.9 (1970-2018)	08.05.21	81.4	1.1
18	Inn-S-chanf	618	2460	38.4 (1998-2021)	25.08.21	25.5	0.7
19	Maggia-Locarno	926	1534	13.8 (1985-2018)	20.05.21	10.8	0.8
20	Rhein-Laufenburg	34040	1078	1522 (1980-1985)	21.07.21	2400	1.6
21	Sihl-Brunau	342	1047	7.83 (1938-2018)	14.07.21	85.8	11.0

b. Radiocarbon signatures

The average $\Delta^{14}\text{C}$ value of POC was $-164.3 \pm 86.2 \text{ ‰}$ ($n = 21$), while average $\Delta^{14}\text{C}$ values for DOC and DIC were $-153.5 \pm 84.7 \text{ ‰}$ and $-166.6 \pm 60.9 \text{ ‰}$, respectively (Table 2 and Figure 2), indicating the presence of pre-aged carbon in all three pools. No samples from the present study yielded $\Delta^{14}\text{C}$ values corresponding to modern (post-bomb) age. The lowest $\Delta^{14}\text{C}$ -value for POC (-446.3 ‰) was measured at station 17 (at Martina) of the Inn River in the Engadin Valley, which is the lowest value (oldest ^{14}C age) of all three carbon pools ($n=63$; Table 2), while the highest PO^{14}C -value (-58.5 ‰) was found at the most downstream site of the Rhine River (station 6 at Weil). DOC $\Delta^{14}\text{C}$ -values ranged from -377.2 ‰ in the upper Rhone River (station 14 at Porte du Scex) to -43.3 ‰ (station 2 of the Thur River at Andelfingen). DIC $\Delta^{14}\text{C}$ -values ranged from -322 ‰ at Martina (station 17) in the lower Engadin to -40.6 ‰ at station 15 (Rhône at Chancy), the latter being the highest value (youngest ^{14}C age) out of all three carbon pools. The amplitude of variability in DIC $\Delta^{14}\text{C}$ values was smaller than for both DOC and

POC, where POC $\Delta^{14}\text{C}$ showed the highest amplitude. In general, $\Delta^{14}\text{C}$ -values of all three carbon phases follow a gradient of decreasing values from north to south. Stations on rivers draining the alpine region in southern Switzerland generally show the lowest $\Delta^{14}\text{C}$ -values, whereas those in the northern part of Switzerland draining the Swiss Plateau are higher.

Table 2: Table about results of ^{14}C for particular (POC) and dissolved (DOC) organic carbon as well as dissolved inorganic carbon (DIC) indicated as $\Delta^{14}\text{C}$ -values.

Station	Name	$\Delta^{14}\text{C}$ -values (‰)		
		PO ^{14}C	DO ^{14}C	DI ^{14}C
1	Rhein-Diepoldsau	-252.3	-278.3	-263.6
2	Thur-Andelfingen	-105.9	-43.3	-138.3
3	Glatt-Rheinsfelden	-142.2	-157.8	-159.8
4	Rhein-Rekingen	-121.6	-87.6	-174.1
5	Birs-Münchenstein	-106.8	-150.4	-119.5
6	Rhein-Basel	-58.5	-132.5	-137.5
7	Aare-BernSchönau	-197.5	-172.1	-171.7
8	Sanne-Gümmenen	-113.7	-67.2	-156.3
9	Aare-Hagneck	-171.8	-117.9	-144.4
10	Aare-Brugg	-91.8	-143.3	-91.8
11	Kleine Emme-Littau	-116.3	-47.5	-162.6
12	Reuss-Mellingen	-157.7	-52.6	-177.4
13	Limmat-Gebenstorf	-193.1	-103.4	-187.7
14	Rhône-Porte du Scex	-217.8	-377.2	-290.5
15	Rhône-Chancy	-257.8	-164.5	-40.6
16	Ticino-Riazzino	-150.2	-258.4	-301.3
17	Inn-Martina	-446.3	-164.0	-125.9
18	Inn-S-chanf	-132.3	-235.2	-207.9
19	Maggia-Locarno	-92.4	-208.4	-131.1
20	Rhein-Laufenburg	-123.7	-76.9	-160.8
21	Sihl-Brunau	-122.0	-185.5	-244.7

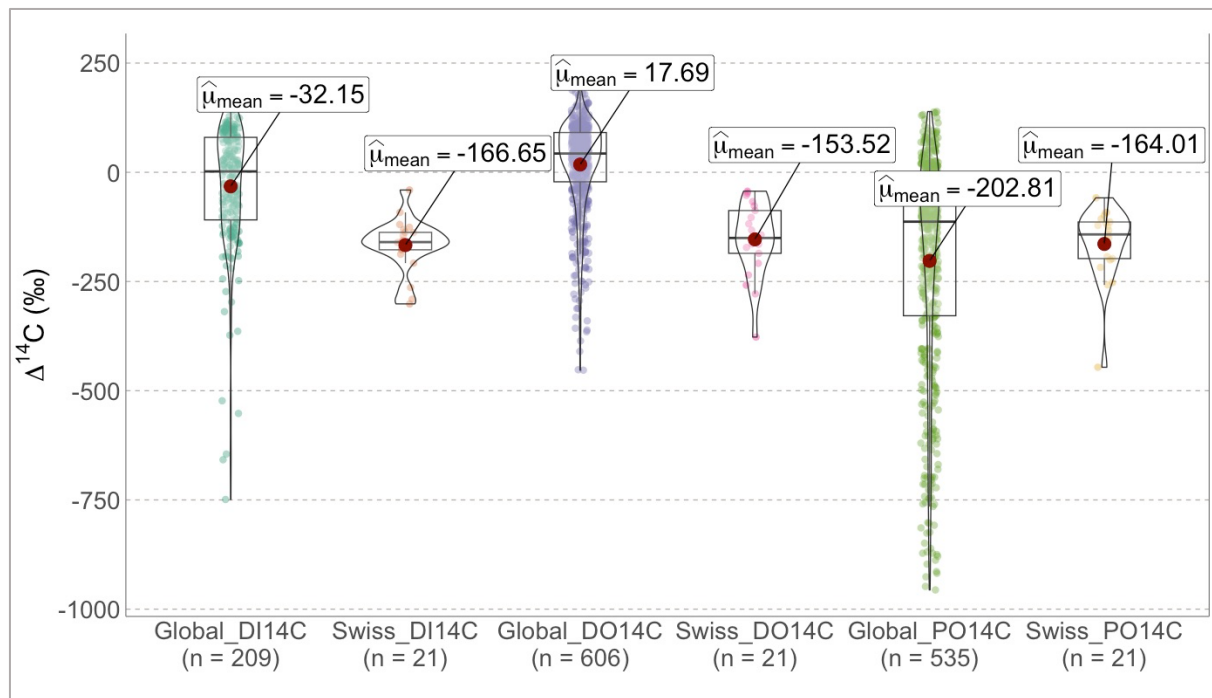


Figure 2: Violin plots of radiocarbon phases ($DI^{14}C$, $DO^{14}C$, $PO^{14}C$) with boxplots showing median values of ^{14}C . Red dots are indicating the mean values. Swiss ^{14}C -phases are compared next to the global compilation from Marwick et al., 2018. Radiocarbon values are expressed in $\Delta^{14}C$ -notation. Points are indicating single measurements.

c. Univariate Regression Analysis

The general outcome of the Pearson correlation plot showed that all three carbon pools ($PO^{14}C$, $DO^{14}C$, $DI^{14}C$) correlate in a similar way regarding their relationships with different parameters (Figure 4). Annual river temperature extracted from the NADUF dataset of the past decade (2012-2020) showed significant negative correlation to $DO^{14}C$ and $DI^{14}C$ ($R^2=0.41$; p-value: < 0.005 and $R^2=0.37$; p-value: < 0.01 , respectively), but not to $PO^{14}C$. Runoff and discharge values corresponding to the sampling day showed no correlation, whereas annual average runoff values extrapolated from the NADUF dataset of the last decade (2012-2020) had a negative correlation with $DI^{14}C$ ($R^2=0.30$; p-value: < 0.05 ; Figure 3). Mean annual basin precipitation (1971-2020) did not show any significant relationships (SI: Table 4).

Regarding topographic features within the catchment basin, mean basin slope showed a significant but weak negative correlation with ^{14}C signatures of $PO^{14}C$ and $DO^{14}C$ ($R^2=0.22$; p-value: < 0.05 ; $R^2=0.37$; p-value: < 0.01 , respectively), but not to $DI^{14}C$. Mean basin elevation shows strongest significant negative correlation with both $PO^{14}C$ and $DO^{14}C$, but not with $DI^{14}C$ ($R^2=0.49$; p-value: < 0.001 , and $R^2=0.39$; p-value: < 0.005 , respectively). No correlation was evident between basin area and any of the ^{14}C -pools (Figure 3). With respect to land-use type, mean basin cover of agricultural fields, which includes farmland, alpine agriculture, as well as pastoral land, exhibits a significant positive

correlation to DO¹⁴C ($R^2=0.47$; p-value: < 0.001). In contrast, there is also a negative correlation between barren areas with PO¹⁴C and DO¹⁴C ($R^2=0.46$; p-value: < 0.001, and $R^2=0.38$; p-value: < 0.005, respectively, Figure 3). For PO¹⁴C only, there was a positive correlation with forest coverage within the catchment ($R^2=0.30$; p-value: < 0.01). Population density did not show any significant relationships with ¹⁴C signatures (SI: Table 4). Concerning bedrock lithology, average basin cover of clastic sediments exhibits a significant positive correlation with DO¹⁴C ($R^2=0.50$; p-value: < 0.001). It should be noted that clastic sediments strongly correlate with agricultural land-use ($R^2=0.63$; p-value: < 0.001). There is also negative correlation of metamorphic rocks and DO¹⁴C ($R^2=0.32$; p-value: < 0.05).

Significant positive correlation was found between DO¹⁴C and DI¹⁴C ($R^2=0.31$; p-value: < 0.01; SI: Table 4), Besides this, there were no other significant correlations between ¹⁴C-values of different carbon phases.

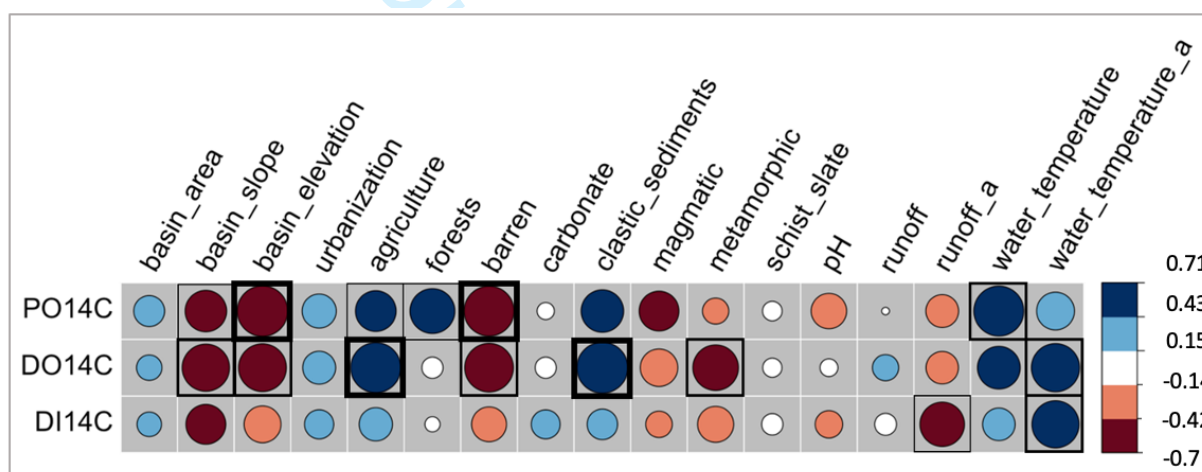


Figure 3: Matrix of Pearson correlation coefficients (r values) between land use, lithology, topography, and water parameters (controls) and radiocarbon values (responses). Circle sizes and colors correspond to the strength of the correlation. Correlations that are significant at the $P = 0.05$, $P = 0.01$, and $P = 0.001$ level are outlined with a thin, regular, and thick black border, respectively. Variables with an “a” at the end indicate annual averages from the past decade extrapolated out from the NADUF data set (2012-2020).

d. *Multivariate Regression Analysis*

The outcome of the redundancy analysis (RDA) shows that two orthogonal axes are explaining a combined 77% of the total sample variation. For the first axis (RDA1: 52%; p-value: < 0.001), parameters such as barren areas, agriculture, catchment slope and elevation are loaded. The second axis (RDA2: 25%; p-value: < 0.1) loads closely with average cover of carbonate rock, forest and pH. As the only significant environmental variable, mean basin elevation seems to exert a major influence on all three carbon phases (p-value: < 0.001). The adjusted R^2 -value of this model is 0.32 (SI: Table 5).

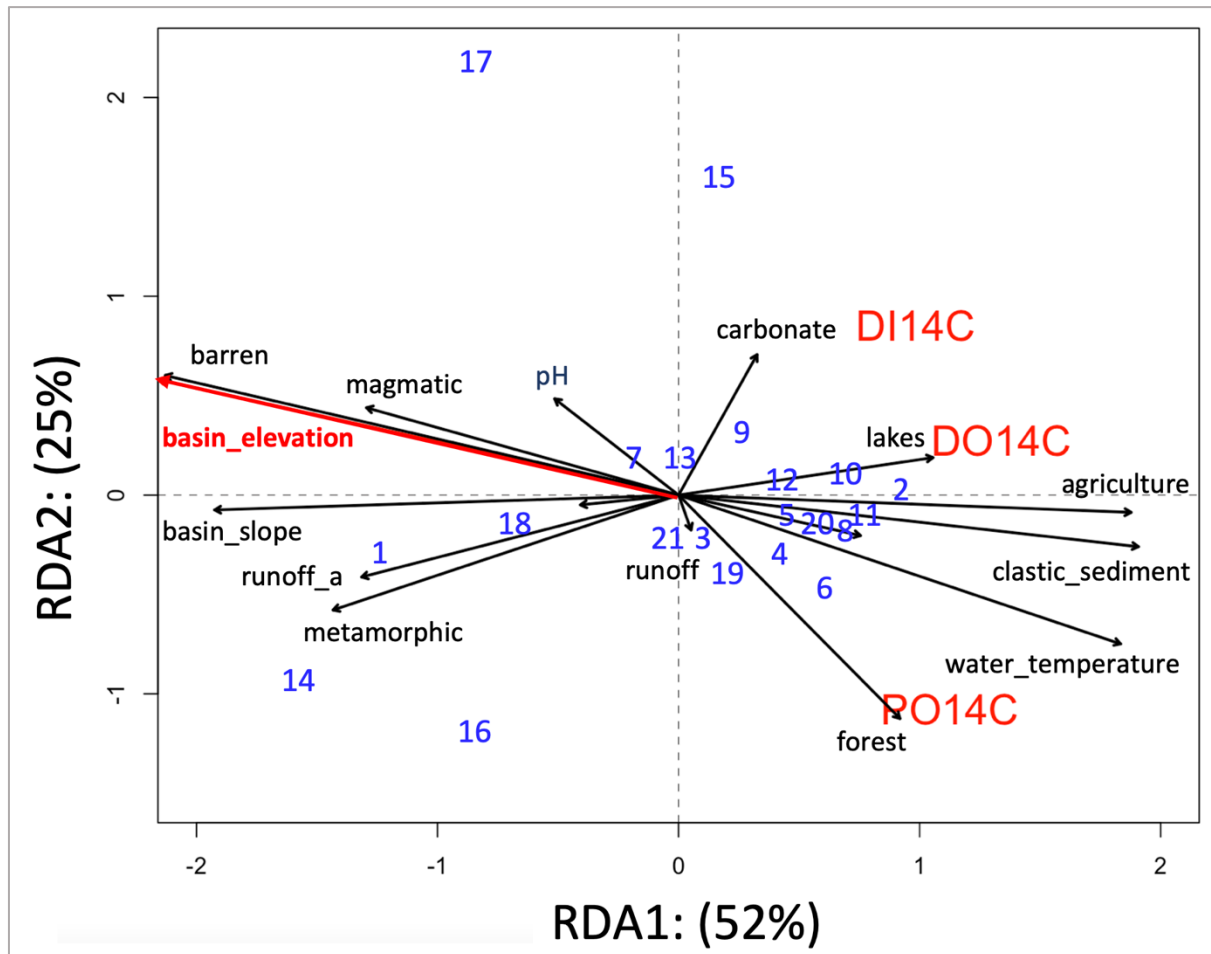


Figure 4: RDA plot showing the RDA1 and RDA2 canonical axes. Environmental control variable loadings are plotted as black arrows where significant vectors are illustrated in red (*basin_elevation*), $PO^{14}C$, $DO^{14}C$, and $DI^{14}C$ response variable loadings are plotted in red, and individual sampling stations (see Table 1,2) are plotted as blue numbers. Variables annotated with an “-a” correspond to annual average values of the past decade (2012-2020).

Discussion

River systems are highly complex and so are the controls on riverine carbon dynamics (Botter et al., 2019; Rodríguez-Murillo et al., 2015; Schwab et al., 2022; Zobrist & Reichert, 2006). The identification of causality drivers of carbon signatures in river systems remains challenging, particularly in complex and heterogeneous landscapes such as those within Switzerland where multiple factors overlap spatially. The 21 rivers across Switzerland cover strong gradients in climate, bedrock, vegetation, and land-use. Samples had been taken as a “snapshot” at high flow, where according to recent studies on Swiss rivers by Gies et al. (2022) and Schwab et al. (2022), POC source apportionment using ^{14}C amongst other parameters into the three main endmembers (vegetation, soil, and bedrock) is most representative when samples are collected during above-average river discharge conditions. The elevated discharge during our sampling meets these conditions. Our observed ^{14}C -values are on the lower end within the global compilation of riverine radiocarbon data (Marwick et al., 2015; Figure 2). While this may partly reflect the different sampling years encompassing both datasets and resulting manifestation of bomb-derived ^{14}C in carbon pools, it is of interest to identify the sources and drivers governing these ^{14}C signatures and their implications for (eco)regional carbon cycling.

Particulate Organic Carbon

Eglinton et al. (2021) showed from ^{14}C measurements of source-specific organic compounds that climate modulation of soil carbon turnover times dictates riverine terrestrial biogenic PO^{14}C values at the global scale. Accordingly, slower soil carbon turnover in alpine settings could thus serve as an explanation for ^{14}C -depleted signature of riverine POC in higher elevation stations. Our study supports this conclusion at the national scale across a pronounced climatic gradient. Riverine POC is depleted in ^{14}C in alpine settings which have higher SOC stocks than lowland soils (Nussbaum et al., 2014). Given the marked differences in climatic regimes among the five different ecoregions, Switzerland might echo global-scale patterns found by Eglinton et al. (2021). In concert with this, temperature, precipitation, and moisture have been identified as major drivers governing SOC (soil organic carbon) stocks in Switzerland (Nussbaum et al., 2014), although other authors have argued that at the regional scale, physiochemical properties (i.e., soil pH, moisture and mineralogy) override the controls of climatic regimes on SOC dynamics in surface soils (González-Domínguez et al., 2019). Additionally, increased soil loss in response to extreme rainfall on Swiss grasslands was observed to occur during July and September, which would coincide with the timeframe of our sampling campaign (Schmidt et al., 2016,

1
2
3 2019). This would lead to increased inputs of pre-aged $PO^{14}C$ from soil erosion, where stable isotopic
4 measurements (^{13}C) are needed to confirm this contribution.
5
6

7 Independent of direct influences of soil-derived carbon inputs and soil turnover times, petrogenic
8 carbon inputs from bedrock weathering and erosion of sedimentary rock mobilized by rain events,
9 freeze-thaw processes, or glacier retreat glaciers are additional potential sources of ancient ^{14}C -free
10 carbon to rivers draining from the alpine terrain. In particular, the terrain above the tree line in the Alps
11 may be comprised of incompletely weathered sedimentary material (Leithold et al., 2006). Steeper
12 slopes erode deeper soil layers where such contributions have been observed to reflect depleted $PO^{14}C$ -
13 values (Van der Voort et al., 2019). The metamorphosed sedimentary rock (schist) called
14 “Bündnerschiefer” outcrops in various watersheds (e.g., Inn and Upper Rhine, could contribute to
15 depleted ^{14}C -values, particularly at station 17 (Martina) in the Engadin, which is surrounded by this type
16 of schist (showed the most depleted $PO^{14}C$ -value). In these alpine regions, further efforts would be
17 needed to distinguish petrogenic POC inputs of fossil age from those derived from pre-aged soil OC.
18
19

20 Downstream in the Swiss Plateau, where ^{14}C -ages are generally younger, $PO^{14}C$ shows a
21 positive correlation to average basin cover of forests, suggesting fresher biospheric C inputs. Storm-
22 facilitated export of carbon has been linked with modern biospheric sources (Goñi et al., 2013; Hilton et
23 al., 2008), where especially during summer months an enhanced contribution of wood-derived POC has
24 been reported in a Swiss catchment (Schwab et al., 2022). The positive correlation of agricultural land-
25 use and $PO^{14}C$ as well as $DO^{14}C$ strongly suggests that the ^{14}C -enriched endmembers of DOC and
26 POC might have a similar origin or mode of supply. Overall, in addition to climatic differences, the stark
27 contrast between Swiss alpine terrain versus Swiss Plateau also reflects a gradient in anthropogenic
28 pressures, contributions from upstream restricted carbon sources, as well as dilution and transformation
29 processes by increased soil, plant biomass inputs and in-stream aquatic productivity (Botter et al., 2019;
30 Schwab et al., 2022; Zobrist et al., 2018).
31
32
33
34
35
36
37
38
39
40
41
42
43
44
45
46
47
48
49
50

51 *Dissolved Organic Carbon*

52 Based on univariate regression analysis, $PO^{14}C$ showed strong negative correlations with
53 several parameters which were also significant for $DO^{14}C$, suggesting some interconnectivity in ^{14}C -
54 depleted carbon inputs from headwater streams. However, there was no significant correlation between
55 the ^{14}C -values of these two carbon phases, implying that they are also influenced by other drivers. As
56 previous studies have observed, ^{14}C -depleted (old) DOC can derive from various sources such as
57
58
59
60

1
2
3 shallow and deep soil layers, groundwater inputs, karst systems, and natural springs, but also from
4 organisms incorporating inorganic carbon from bedrock weathering (Raymond & Bauer, 2004; You et
5 al., 2022). A single source input process of old POC (e.g., erosion of rock or pre-aged soils), in contrast
6
7 to multiple sources input processes of pre-aged DOC (e.g., soil leaching, in-stream productivity,
8
9 groundwater, and glacial meltwater inputs) could explain such an overlapping trend, while also
10
11 reconciling the lack of relationship between PO^{14}C and DO^{14}C .
12
13

14
15 It has been argued that in-stream productivity of major lowland rivers, where flow velocities are
16 low, are significant contributors of riverine organic carbon (Chen et al., 2022; You et al., 2022). Moreover,
17
18 Chen et al. (2022) recently suggested that even in mountainous rivers in-stream production and
19 transformation of carbon exerts a significant influence on riverine DO^{14}C -dynamics. Riverine in-stream
20 processes can be separated into biotic (e.g., biodegradation and primary production) or abiotic (e.g.,
21 absorption, desorption, photo-oxidation, dissolution), which are each strongly controlled by river water
22 temperature and residence time (Catalán et al., 2016; Chen et al., 2022; You et al., 2022). The significant
23 positive relationship between DO^{14}C and the long-term average of annual river water temperature from
24 the NADUF dataset supports the assumption of significant in-stream productivity. However, such long-
25 term trends in river water temperature almost certainly also reflect similar trends in air and land surface
26 temperature, with attendant changes in terrestrial productivity and soil DOC dynamics. Enhanced DOC
27 leaching from soils was observed particularly when increased precipitation was coupled with increasing
28 soil temperatures, highlighted by an in-situ soil warming study as well as a recent laboratory study
29 (Hagedorn et al., 2010; Schindlbacher et al., 2019). Consequently, it remains challenging to attribute
30 the links in river DO^{14}C solely to aquatic productivity, and further information (e.g., stable carbon isotope
31 as well as other geochemical data) would help to distinguish biospheric from petrogenic contributions,
32 as well as allochthonous from autochthonous sources. DOC in lowland rivers is often derived from
33 fresh vegetation or soil leaching, thus ubiquitously young (enriched in ^{14}C) (Marwick et al., 2015).
34
35 Agricultural farmlands could enhance this input of fresh carbon through fresh crops or even inputs of
36 manure. Studies have pointed out that excessive inputs of manures from pastoral activities can lead to
37 eutrophication excessively increasing in-stream productivity (Brailsford et al., 2019; Stumpe &
38 Marschner, 2010), which can lead to younger DO^{14}C -ages. It has also been argued that agricultural
39 practices could supply ^{14}C -depleted DOC to rivers by the exhumation of deeper soil layers following
40 conversion of forests to cropland (which increases soil erosion due to weaker soil stability with less
41 extensive root systems; Butman et al., 2015; Lambert et al., 2017). Compared to signatures emanating
42
43
44
45
46
47
48
49
50
51
52
53
54
55
56
57
58
59
60

1
2
3 from upland regions of Swiss rivers, such level of ^{14}C -depletion in DOC is relatively modest and
4 contributions would correspond to younger DO^{14}C ages (higher DO^{14}C values) (Barnes et al., 2018;
5 Butman et al., 2012; Butman et al., 2015) given that Swiss riverine DOC generally exhibits relatively low
6 ^{14}C values compared to the global average (Marwick et al., 2015; Raymond et al., 2004).
7
8
9

10 11 12 *Dissolved Inorganic Carbon*

13
14 Of the three carbon phases DI^{14}C exhibits the fewest significant univariate relationships to
15 watershed variables. This renders it difficult to pinpoint its source, especially given the complex nature
16 of weathering-related interactions between the bedrock and atmosphere. Swiss rivers are oversaturated
17 with respect to atmospheric CO_2 primarily as a consequence of weathering of carbonate lithologies. This
18 results in a net outgassing of CO_2 (Zobrist et al., 2018). In contrast, increased runoff from snow and ice
19 melt can lead to an undersaturation of DIC in rivers, and consequently to atmospheric CO_2 absorption
20 (Zobrist et al., 2018). Invasion of atmospheric CO_2 (enriched in ^{14}C) into rivers could possibly dilute
21 chemically weathered DIC ^{14}C signatures (depleted in ^{14}C). Thus, the identification of drivers can be
22 complicated depending on the degree of oversaturation or undersaturation of the river.
23
24
25
26
27
28
29
30

31
32 There was no significant correlation between DI^{14}C and carbonate lithology or any other broad
33 type of lithological category included in our analysis. The argument that DI^{14}C is foremost governed by
34 kinetics (e.g., temperature) rather than lithology or land-use, would explain this lack of correlation with
35 watershed variables. Further measurements are necessary to deconvolute signatures, and apportion
36 specific contributions (Blattmann et al., 2019; Zobrist et al., 2018).
37
38
39
40

41
42 In contrast to the organic carbon phases, DI^{14}C did exhibit a significant negative correlation with
43 average runoff of the past 9-years (2012-2020). This goes in concert with an in-situ field experiment and
44 recent laboratory study showing especially increased precipitation but also coupled with soil warming
45 leading to enhances soil DIC leaching (Hagedorn et al., 2010; Schindlbacher et al., 2019). Our finding
46 that DI^{14}C and average runoff of the past decades (1971-2020) showed a significant correlation suggests
47 a link with the small but significant increase in DIC concentration during the past 4 decades in all four
48 major Swiss river systems (Rhine, Rhone, Ticino, and Inn) (Zobrist et al., 2018). Over the same time-
49 period, carbonate lithology-related parameters such as alkalinity, total hardness, Ca and Mg have
50 increased by up to 10% (Zobrist et al., 2018), thus suggesting a higher proportion of DIC from carbonate
51 weathering that is depleted in ^{14}C . As DIC can be degassed from rivers to the atmosphere, coupled with
52
53
54
55
56
57
58
59
60

the long-term increases of DIC concentration observed in major Swiss rivers (Zobrist et al., 2018), such processes could pose significant positive feedback to climate change.

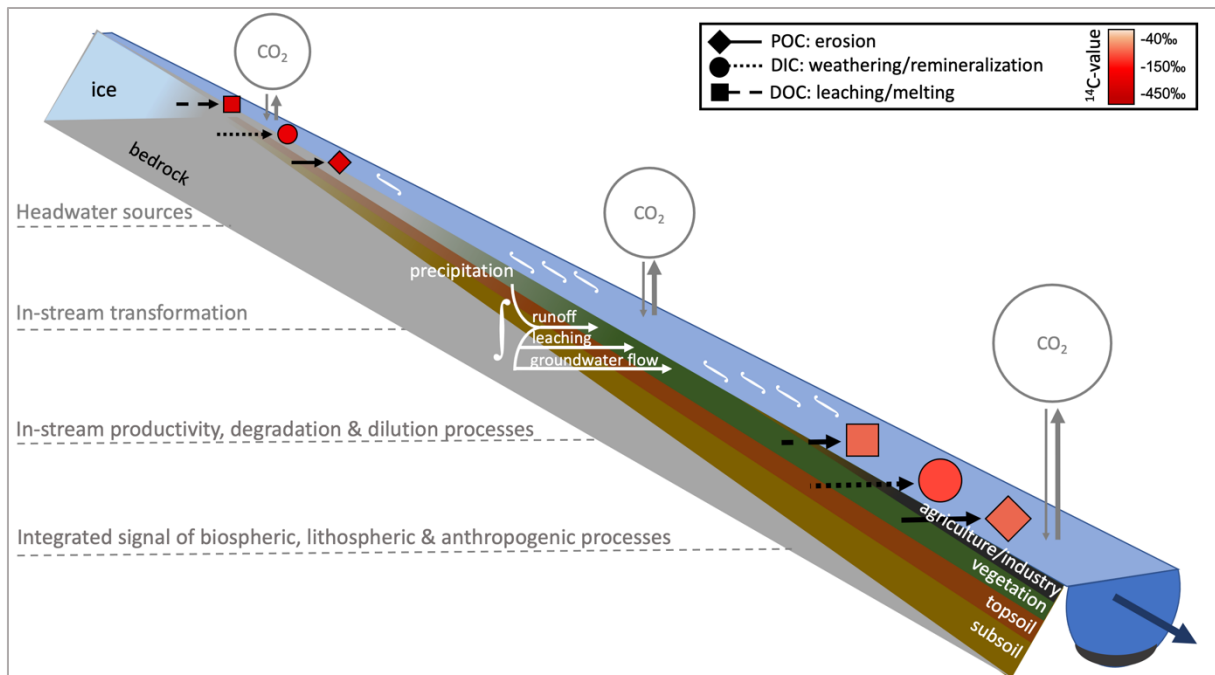


Figure 5: Conceptual figure summarizing the main findings of this study. The river from headwater to downstream is illustrated with different processes occurring along the continuum. Different shapes representing carbon phases (POC, DOC, DIC) are illustrated and colored to approximate the average $\Delta^{14}\text{C}$ -value (legend) for stations draining alpine terrain (upper left) and plateau (lower right). Arrows indicate riverine input processes and major sources). Symbol and arrow sizes provide an indication of the magnitude C inputs and pools. The white arrows and integral sign illustrate the hydrological processes (mainly driven by precipitation) that deliver carbon to the river network. Contributions from major terrestrial C-sources (ice, bedrock, top- & sub-soil, vegetation, agriculture and industry) are also shown.

In our study we note that DIC is more enriched in ^{14}C in the Swiss Plateau, which also positively correlated to DO^{14}C -values. Coupled effects of precipitation and warming (Schindlbacher et al., 2019) as well as microbial decomposition accelerated by increased OC inputs due to agricultural practices might be an explanation for such an observation. Comparing headwaters to downstream sampling sites, decreasing contributions of upstream restricted carbon sources, as well as dilution and transformation processes by increased biospheric inputs might explain this pattern (Botter et al., 2019; Schwab et al., 2022; Zobrist et al., 2018). This younger DI^{14}C -signature in the Swiss Plateau compared to the Swiss Alps possibly originates from enhanced soil organic matter respiration and DIC leaching and could override the “alpine characteristic” DI^{14}C -signatures further downstream. Additionally, the oversaturation of Swiss rivers with respect to DIC can lead to the outgassing of headwater sourced ^{14}C -depleted CO_2 during downstream transport, while subsequent atmospheric CO_2 uptake or DIC emanating from more

1
2
3 modern sources further downstream could lead to dilution of signals from bedrock weathering and
4 related processes (Zobrist et al., 2018). Nevertheless, considering the rate of change in ^{14}C
5 characteristics of the two other carbon pools (POC, DOC), the difference in DI^{14}C -values from
6 headwaters to downstream is relatively modest.
7
8
9

10 11 12 13 *Conclusion*

14
15 All three riverine carbon phases become increasingly enriched in ^{14}C from high elevation regions
16 in the Alps towards the Swiss Plateau, which may reflect either preferential removal of ^{14}C -depleted
17 carbon or dilution by fresh carbon from in-stream processes or inputs along the riverine continuum
18 (Figure 5). Redundancy analysis (RDA) underlines this main observation as mean basin elevation is
19 associated negatively with $\Delta^{14}\text{C}$ of all three riverine C phases (Figure 4). Downstream, on the Swiss
20 Plateau, agricultural land-use seems to promote higher $\Delta^{14}\text{C}$ -values, and it is notable that stations which
21 are strongly impacted by intensive agricultural land-use (2, 8, and 11) exhibit very similar ^{14}C -values in
22 all three carbon phases. This might indicate an overriding influence of agricultural practices on riverine
23 ^{14}C -values. The controls on DI^{14}C -dynamics, however, appear more complex. Since these major
24 controls fall within the gradient between Alpine ecoregions and the Swiss Plateau, where covariation of
25 multiple variables exists (e.g., elevation, barren surfaces, slope, agriculture, clastic sediments),
26 disentanglement of the governing controls on ^{14}C -dynamics in Swiss river systems remains challenging.
27 For example, hydrological controls such as discharge and runoff do not emerge as major factors
28 governing ^{14}C -values of POC and DOC across Switzerland yet exhibit correlations with DI^{14}C . As this
29 study includes only a single “snapshot” for each river during the summer high-flow conditions, we are
30 unable to assess potential influences of seasonality and hydrological variability on ^{14}C signatures.
31 Comparing our dataset obtained during a year of above-average discharge condition with those for other
32 years as well as seasonal time-series, may help to improve the understanding of long-term effects of
33 climate and land-use change on Swiss rivers in the Anthropocene.
34
35
36
37
38
39
40
41
42
43
44
45
46
47
48
49
50
51
52
53
54
55
56
57
58
59
60

References

- Amundson, R., Berhe, A. A., Hopmans, J. W., Olson, C., Sztein, A. E., & Sparks, D. L. (2015). Soil and human security in the 21st century. In *Science* (Vol. 348, Issue 6235). American Association for the Advancement of Science. <https://doi.org/10.1126/science.1261071>
- Aufdenkampe, A. K., Mayorga, E., Raymond, P. A., Melack, J. M., Doney, S. C., Alin, S. R., Aalto, R. E., & Yoo, K. (2011). Riverine coupling of biogeochemical cycles between land, oceans, and atmosphere. *Frontiers in Ecology and the Environment*, 9(1), 53–60. <https://doi.org/10.1890/100014>
- Barnes, R. T., Butman, D. E., Wilson, H. F., & Raymond, P. A. (2018). Riverine Export of Aged Carbon Driven by Flow Path Depth and Residence Time. *Environmental Science and Technology*, 52(3), 1028–1035. <https://doi.org/10.1021/acs.est.7b04717>
- Battin, T. J., Luysaert, S., Kaplan, L. A., Aufdenkampe, A. K., Richter, A., & Tranvik, L. J. (2009). The boundless carbon cycle. In *Nature Geoscience* (Vol. 2, Issue 9, pp. 598–600). <https://doi.org/10.1038/ngeo618>
- Blattmann, T. M., Wang, S. L., Lupker, M., Märki, L., Haghypour, N., Wacker, L., Chung, L. H., Bernasconi, S. M., Plötze, M., & Eglinton, T. I. (2019). Sulphuric acid-mediated weathering on Taiwan buffers geological atmospheric carbon sinks. *Scientific Reports*, 9(1). <https://doi.org/10.1038/s41598-019-39272-5>
- Bolliger, J., Hagedorn, F., Leifeld, J., Böhl, J., Zimmermann, S., Soliva, R., & Kienast, F. (2008). Effects of land-use change on carbon stocks in Switzerland. *Ecosystems*, 11(6), 895–907. <https://doi.org/10.1007/s10021-008-9168-6>
- Botter, M., Burlando, P., & Fatichi, S. (2019). Anthropogenic and catchment characteristic signatures in the water quality of Swiss rivers: A quantitative assessment. *Hydrology and Earth System Sciences*, 23(4), 1885–1904. <https://doi.org/10.5194/hess-23-1885-2019>
- Brailesford, F. L., Glanville, H. C., Golyshein, P. N., Johnes, P. J., Yates, C. A., & Jones, D. L. (2019). Microbial uptake kinetics of dissolved organic carbon (DOC) compound groups from river water and sediments. *Scientific Reports*, 9(1), 11229. <https://doi.org/10.1038/s41598-019-47749-6>
- Butman, D. E., Wilson, H. F., Barnes, R. T., Xenopoulos, M. A., & Raymond, P. A. (2015). Increased mobilization of aged carbon to rivers by human disturbance. *Nature Geoscience*, 8(2), 112–116. <https://doi.org/10.1038/ngeo2322>
- Butman, D., Raymond, P. A., Butler, K., & Aiken, G. (2012). Relationships between $\delta^{14}\text{C}$ and the molecular quality of dissolved organic carbon in rivers draining to the coast from the conterminous United States. *Global Biogeochemical Cycles*, 26(4). <https://doi.org/10.1029/2012GB004361>
- Catalán, N., Marcé, R., Kothawala, D. N., & Tranvik, L. J. (2016). Organic carbon decomposition rates controlled by water retention time across inland waters. *Nature Geoscience*, 9(7), 501–504. <https://doi.org/10.1038/ngeo2720>
- Chen, S., Zhong, J., Ran, L., Yi, Y., Wang, W., Yan, Z., Li, S., & Mostafa, K. M. G. (2022). Geographical controls and anthropogenic impacts on dissolved organic carbon from mountainous rivers: Insights from optical properties and carbon isotopes. <https://doi.org/10.5194/bg-2022-217>
- Cole, J. J., Prairie, Y. T., Caraco, N. F., McDowell, W. H., Tranvik, L. J., Striegl, R. G., Duarte, C. M., Kortelainen, P., Downing, J. A., Middelburg, J. J., & Melack, J. (2007). Plumbing the global carbon cycle: Integrating inland waters into the terrestrial carbon budget. *Ecosystems*, 10(1), 171–184. <https://doi.org/10.1007/s10021-006-9013-8>
- Draper, N. R. (2002). Applied regression analysis bibliography update 2000-2001. *Communications in Statistics - Theory and Methods*, 31(11), 2051. <https://doi.org/10.1081/STA-120015017>
- Eglinton, T. I., Galy, V. v., Hemingway, J. D., Feng, X., Bao, H., Blattmann, T. M., Dickens, A. F., Gies, H., Giosan, L., Haghypour, N., Hou, P., Lupker, M., McIntyre, C. P., Montluçon, D. B., Peucker-Ehrenbrink, B., Ponton, C., Schefuß, E., Schwab, M. S., Voss, B. M., ... Zhao, M. (2021). Climate control on terrestrial biospheric carbon turnover. 118. <https://doi.org/10.1073/pnas.2011585118-DCSupplemental>
- Ellis, E. E., Keil, R. G., Ingalls, A. E., Richey, J. E., & Alin, S. R. (2012). Seasonal variability in the sources of particulate organic matter of the Mekong River as discerned by elemental and lignin analyses. *Journal of Geophysical Research: Biogeosciences*, 117(1). <https://doi.org/10.1029/2011JG001816>
- Friedlingstein, P., Jones, M. W., O'Sullivan, M., Andrew, R. M., Bakker, D. C. E., Hauck, J., le Quéré, C., Peters, G. P., Peters, W., Pongratz, J., Sitch, S., Canadell, J. G., Ciais, P., Jackson, R. B., Alin, S. R., Anthoni, P., Bates, N. R., Becker, M., Bellouin, N., ... Zeng, J. (2022). Global Carbon Budget 2021. *Earth System Science Data*, 14(4), 1917–2005. <https://doi.org/10.5194/essd-14-1917-2022>
- FOEN:<https://data.geo.admin.ch/ch.swisstopo.geologie-geotechnik-gk500-genese/>
- FOEN:<https://www.bfs.admin.ch/bfs/de/home/dienstleistungen/geostat/geodaten-bundesstatistik/boden-nutzung-bedeckung-eignung/arealstatistik-schweiz.assetdetail.20104753.html>
- Gaillardet, J., Calmels, D., Romero-Mujalli, G., Zakharova, E., & Hartmann, J. (2019). Global climate control on carbonate weathering intensity. *Chemical Geology*, 527. <https://doi.org/10.1016/j.chemgeo.2018.05.009>
- Galy, V., Eglinton, T., France-Lanord, C., & Sylva, S. (2011). The provenance of vegetation and environmental signatures encoded in vascular plant biomarkers carried by the Ganges-Brahmaputra rivers. *Earth and Planetary Science Letters*, 304(1–2), 1–12. <https://doi.org/10.1016/j.epsl.2011.02.003>
- Galy, V., Peucker-Ehrenbrink, B., & Eglinton, T. (2015). Global carbon export from the terrestrial biosphere controlled by erosion. *Nature*, 521(7551), 204–207. <https://doi.org/10.1038/nature14400>
- Gies, H., Lupker, M., Wick, S., Haghypour, N., Buggle, B., & Eglinton, T. (2022). Discharge-Modulated Soil Organic Carbon Export From Temperate Mountainous Headwater Streams. *Journal of Geophysical Research: Biogeosciences*, 127(3). <https://doi.org/10.1029/2021JG006624>
- Goñi, M. A., Hatten, J. A., Wheatcroft, R. A., & Borgeld, J. C. (2013). Particulate organic matter export by two contrasting small mountainous rivers from the Pacific Northwest, U.S.A. *Journal of Geophysical Research: Biogeosciences*, 118(1), 112–134. <https://doi.org/10.1002/jgrg.20024>
- González-Domínguez, B., Niklaus, P. A., Studer, M. S., Hagedorn, F., Wacker, L., Haghypour, N., Zimmermann, S., Walthert, L., McIntyre, C., & Abiven, S. (2019). Temperature and moisture are minor drivers of regional-scale soil organic carbon dynamics. *Scientific Reports*, 9(1). <https://doi.org/10.1038/s41598-019-42629-5>

- 1
2
3 Gudmundsson, L., Boulange, J., Do, H. X., Gosling, S. N., Grillakis, M. G., Koutroulis, A. G., Leonard, M., Liu, J., Schmied, H. M.,
4 Papadimitriou, L., Pokhrel, Y., Seneviratne, S. I., Satoh, Y., Thiery, W., Westra, S., & Zhang, X. (n.d.). *Globally observed trends*
5 *in mean and extreme river flow attributed to climate change*. <https://doi.org/10.1594/PANGAEA.887470>
- 6 Hagedorn, F., Krause, H.-M., Studer, M., Schellenberger, A., & Gattinger, A. (2018). *Boden und Umwelt Organische Bodensubstanz,*
7 *Treibhausgasemissionen und physikalische Belastung von Schweizer Böden*.
- 8 Hagedorn, F., Martin, M., Rixen, C., Rusch, S., Bebi, P., Zürcher, A., Siegwolf, R. T. W., Wipf, S., Escape, C., Roy, J., & Hättenschwiler,
9 S. (2010). Short-term responses of ecosystem carbon fluxes to experimental soil warming at the Swiss alpine treeline.
10 *Biogeochemistry*, 97(1), 7–19. <https://doi.org/10.1007/s10533-009-9297-9>
- 11 Harris, R. M. B., Beaumont, L. J., Vance, T. R., Tozer, C. R., Remenyi, T. A., Perkins-Kirkpatrick, S. E., Mitchell, P. J., Nicotra, A. B.,
12 McGregor, S., Andrew, N. R., Letnic, M., Kearney, M. R., Wernberg, T., Hutley, L. B., Chambers, L. E., Fletcher, M. S., Keatley,
13 M. R., Woodward, C. A., Williamson, G., ... Bowman, D. M. J. S. (2018). Biological responses to the press and pulse of climate
14 trends and extreme events. In *Nature Climate Change* (Vol. 8, Issue 7, pp. 579–587). Nature Publishing Group.
15 <https://doi.org/10.1038/s41558-018-0187-9>
- 16 Hemingway, J. D., Schefuß, E., Spencer, R. G. M., Dinga, B. J., Eglinton, T. I., McIntyre, C., & Galy, V. v. (2017). Hydrologic controls on
17 seasonal and inter-annual variability of Congo River particulate organic matter source and reservoir age. *Chemical Geology*, 466,
18 454–465. <https://doi.org/10.1016/j.chemgeo.2017.06.034>
- 19 Hilton, R. G., Galy, A., Hovius, N., Chen, M. C., Horng, M. J., & Chen, H. (2008). Tropical-cyclone-driven erosion of the terrestrial
20 biosphere from mountains. *Nature Geoscience*, 1(11), 759–762. <https://doi.org/10.1038/ngeo333>
- 21 Hilton, R. G., Galy, A., Hovius, N., Horng, M. J., & Chen, H. (2011). Efficient transport of fossil organic carbon to the ocean by steep
22 mountain rivers: An orogenic carbon sequestration mechanism. *Geology*, 39(1), 71–74. <https://doi.org/10.1130/G31352.1>
- 23 Horan, K., Hilton, R. G., Dellinger, M., Tipper, E., Galy, V., Calmels, D., Selby, D., Gaillardet, J., Ottley, C. J., Parsons, D. R., & Burton,
24 K. W. (2019). Carbon dioxide emissions by rock organic carbon oxidation and the net geochemical carbon budget of the Mackenzie
25 River Basin. *American Journal of Science*, 319(6), 473–499. <https://doi.org/10.2475/06.2019.02>
- 26 Kao, S. J., Hilton, R. G., Selvaraj, K., Dai, M., Zehetner, F., Huang, J. C., Hsu, S. C., Sparkes, R., Liu, J. T., Lee, T. Y., Yang, J. Y. T.,
27 Galy, A., Xu, X., & Hovius, N. (2014). Preservation of terrestrial organic carbon in marine sediments offshore Taiwan: Mountain
28 building and atmospheric carbon dioxide sequestration. *Earth Surface Dynamics*, 2(1), 127–139. <https://doi.org/10.5194/esurf-2-127-2014>
- 29 Keil, R. G., Mayer, L. M., Quay, P. D., Richey, J. E., & Hedges, J. I. (1997). Loss of organic matter from riverine particles in deltas. In
30 *Geochimica et Cosmochimica Acta* (Vol. 61, Issue 7).
- 31 Kelsey, S. A., Grottoili, A. G., Bauer, J. E., Lorenz, K., Lal, R., Matsui, Y., & Huey-Sanders, T. M. (2020). Effects of agricultural and tillage
32 practices on isotopic signatures and fluxes of organic and inorganic carbon in headwater streams. *Aquatic Sciences*, 82(2).
33 <https://doi.org/10.1007/s00027-019-0691-7>
- 34 Lambert, T., Bouillon, S., Darchambeau, F., Morana, C., Roland, F. A. E., Descy, J. P., & Borges, A. v. (2017). Effects of human land
35 use on the terrestrial and aquatic sources of fluvial organic matter in a temperate river basin (The Meuse River, Belgium).
36 *Biogeochemistry*, 136(2), 191–211. <https://doi.org/10.1007/s10533-017-0387-9>
- 37 Lang, S. Q., McIntyre, C. P., Bernasconi, S. M., Früh-Green, G. L., Voss, B. M., Eglinton, T. I., & Wacker, L. (2016). Rapid14c analysis
38 of dissolved organic carbon in non-saline waters. *Radiocarbon*, 58(3), 505–515. <https://doi.org/10.1017/RDC.2016.17>
- 39 Leifeld, J., Bassin, S., & Fuhrer, J. (2005). Carbon stocks in Swiss agricultural soils predicted by land-use, soil characteristics, and
40 altitude. *Agriculture, Ecosystems and Environment*, 105(1–2), 255–266. <https://doi.org/10.1016/j.agee.2004.03.006>
- 41 Leifeld, J., Zimmermann, M., Fuhrer, J., & Conen, F. (2009). Storage and turnover of carbon in grassland soils along an elevation gradient
42 in the Swiss Alps. *Global Change Biology*, 15(3), 668–679. <https://doi.org/10.1111/j.1365-2486.2008.01782.x>
- 43 Levin, I., & Hesshaimer, V. (2000). Radiocarbon - A unique tracer of global carbon cycle dynamics. In *Radiocarbon* (Vol. 42, Issue 1, pp.
44 69–80). University of Arizona. <https://doi.org/10.1017/S0033822200053066>
- 45 Liu, J., You, Y., Li, J., Sitch, S., Gu, X., Nabel, J. E. M. S., Lombardozi, D., Luo, M., Feng, X., Arneith, A., Jain, A. K., Friedlingstein, P.,
46 Tian, H., Poulter, B., & Kong, D. (2021). Response of global land evapotranspiration to climate change, elevated CO₂, and land
47 use change. *Agricultural and Forest Meteorology*, 311. <https://doi.org/10.1016/j.agrformet.2021.108663>
- 48 Marwick, T. R., Tamooh, F., Teodoru, C. R., Borges, A. v., Darchambeau, F., & Bouillon, S. (2015). The age of river-transported carbon:
49 A global perspective. *Global Biogeochemical Cycles*, 29(2), 122–137. <https://doi.org/10.1002/2014GB004911>
- 50 Mccallister, S. L., Bauer, J. E., Cherrier, J. E., & Ducklow, H. W. (2004). Assessing sources and ages of organic matter supporting river
51 and estuarine bacterial production: A multiple-isotope (14 C, 13 C, and 15 N) approach. In *Limnol. Oceanogr* (Vol. 49, Issue 5).
52 <http://waterdata.usgs>.
- 53 McIntyre, C. P., Wacker, L., Haghpor, N., Blattmann, T. M., Fahrni, S., Usman, M., Eglinton, T. I., & Synal, H. A. (2017). Online 13C
54 and 14C Gas Measurements by EA-IRMS-AMS at ETH Zürich. *Radiocarbon*, 59(3), 893–903.
55 <https://doi.org/10.1017/RDC.2016.68>
- 56 NADUF: <https://opendata.eawag.ch/group/naduf-national-long-term-surveillance-of-swiss-rivers>
- 57 Nussbaum, M., Papritz, A., Baltensweiler, A., & Walthert, L. (2014). Estimating soil organic carbon stocks of Swiss forest soils by robust
58 external-drift kriging. *Geoscientific Model Development*, 7(3), 1197–1210. <https://doi.org/10.5194/gmd-7-1197-2014>
- 59 *Publ Aqua 2022 copy*. (n.d.).
- 60 Quéré, C., Andrew, R., Friedlingstein, P., Sitch, S., Hauck, J., Pongratz, J., Pickers, P., Ivar Korsbakken, J., Peters, G., Canadell, J.,
Arneith, A., Arora, V., Barbero, L., Bastos, A., Bopp, L., Ciais, P., Chini, L., Ciais, P., Doney, S., ... Zheng, B. (2018). Global Carbon
Budget 2018. *Earth System Science Data*, 10(4), 2141–2194. <https://doi.org/10.5194/essd-10-2141-2018>
- Ran, L., Tian, M., Fang, N., Wang, S., Lu, X., Yang, X., & Cho, F. (2018). Riverine carbon export in the arid to semiarid Wuding River
catchment on the Chinese Loess Plateau. *Biogeosciences*, 15(12), 3857–3871. <https://doi.org/10.5194/bg-15-3857-2018>
- Raymond, P. A., & Bauer, J. E. (2001). *Use of 14 C and 13 C natural abundances for evaluating riverine, estuarine, and coastal DOC*
and POC sources and cycling: a review and synthesis. www.elsevier.nl/locate/orggeochem
- Raymond, P. A., Bauer, J. E., Caraco, N. F., Cole, J. J., Longworth, B., & Petsch, S. T. (2004). Controls on the variability of organic
matter and dissolved inorganic carbon ages in northeast US rivers. *Marine Chemistry*, 92(1-4 SPEC. ISS.), 353–366.
<https://doi.org/10.1016/j.marchem.2004.06.036>

- 1
2
3 Raymond, P. A., Oh, N. H., Turner, R. E., & Broussard, W. (2008). Anthropogenically enhanced fluxes of water and carbon from the
4 Mississippi River. *Nature*, *451*(7177), 449–452. <https://doi.org/10.1038/nature06505>
- 5 Raymond, P. A., Saiers, J. E., & Sobczak, W. v. (2016). Hydrological and biogeochemical controls on watershed dissolved organic matter
6 transport: pulse-shunt concept. In *CONCEPTS & SYNTHESIS EMPHASIZING NEW IDEAS TO STIMULATE RESEARCH IN*
7 *ECOLOGY Ecology* (Vol. 97, Issue 1). <http://www.horizon-systems.com/nhdplus/>
- 8 Regnier, P., Friedlingstein, P., Ciais, P., Mackenzie, F. T., Gruber, N., Janssens, I. A., Laruelle, G. G., Lauerwald, R., Luysaert, S.,
9 Andersson, A. J., Arndt, S., Arnosti, C., Borges, A. v., Dale, A. W., Gallego-Sala, A., Godd ris, Y., Goossens, N., Hartmann, J.,
10 Heinze, C., ... Thullner, M. (2013). Anthropogenic perturbation of the carbon fluxes from land to ocean. *Nature Geoscience*, *6*(8),
11 597–607. <https://doi.org/10.1038/ngeo1830>
- 12 Regnier, P., Resplandy, L., Najjar, R. G., & Ciais, P. (2022). The land-to-ocean loops of the global carbon cycle. In *Nature* (Vol. 603,
13 Issue 7901, pp. 401–410). Nature Research. <https://doi.org/10.1038/s41586-021-04339-9>
- 14 Tittel, J., Musolf, A., Rinke, K., & B tner, O. (2022). Anthropogenic Transformation Disconnects a Lowland River From Contemporary
15 Carbon Stores in Its Catchment. *Ecosystems*, *25*. <https://doi.org/10.1007/s10021-021-0067>
- 16 Ripple, W. J., Wolf, C., Gregg, J. W., Levin, K., Rockstr m, J., Newsome, T. M., Betts, M. G., Huq, S., Law, B. E., Kemp, L., Kalmus, P.,
17 & Lenton, T. M. (2022). World Scientists' Warning of a Climate Emergency 2022. *BioScience*.
18 <https://doi.org/10.1093/biosci/biac083>
- 19 Rodriguez-Murillo, J. C., Zobrist, J., & Filella, M. (2015). Temporal trends in organic carbon content in the main Swiss rivers, 1974-2010.
20 *Science of the Total Environment*, *502*, 206–217. <https://doi.org/10.1016/j.scitotenv.2014.08.096>
- 21 Schindlbacher, A., Beck, K., Holzheu, S., & Borken, W. (2019). Inorganic Carbon Leaching From a Warmed and Irrigated Carbonate
22 Forest Soil. *Frontiers in Forests and Global Change*, *2*. <https://doi.org/10.3389/ffgc.2019.00040>
- 23 Schmidt, S., Alewell, C., & Meusburger, K. (2019). Monthly RUSLE soil erosion risk of Swiss grasslands. *Journal of Maps*, *15*(2), 247–
24 256. <https://doi.org/10.1080/17445647.2019.1585980>
- 25 Schmidt, S., Alewell, C., Panagos, P., & Meusburger, K. (2016). Regionalization of monthly rainfall erosivity patterns in Switzerland.
26 *Hydrology and Earth System Sciences*, *20*(10), 4359–4373. <https://doi.org/10.5194/hess-20-4359-2016>
- 27 Schuur, E. A. G., Druffel, E. R. M., & Trumbore Editors, S. E. (2016). *Radiocarbon and Climate Change Mechanisms, Applications and*
28 *Laboratory Techniques*.
- 29 Schwab, M. S., Gies, H., Freymond, C. V., Lupker, M., Haghypour, N., & Eglinton, T. I. (2022). Environmental and hydrologic controls on
30 sediment and organic carbon export from a subalpine catchment: insights from a time series. *Biogeosciences*, *19*(23), 5591–5616.
31 <https://doi.org/10.5194/bg-19-5591-2022>
- 32 Stumpe, B., & Marschner, B. (2010). Dissolved organic carbon from sewage sludge and manure can affect estrogen sorption and
33 mineralization in soils. *Environmental Pollution*, *158*(1), 148–154. <https://doi.org/10.1016/j.envpol.2009.07.027>
- 34 Syvitski, J. P. M. (2003). Supply and flux of sediment along hydrological pathways: Research for the 21st century. *Global and Planetary*
35 *Change*, *39*(1–2), 1–11. [https://doi.org/10.1016/S0921-8181\(03\)00008-0](https://doi.org/10.1016/S0921-8181(03)00008-0)
- 36 Szidat, S., Jenk, T. M., Synal, H.-A., Kalberer, M., Wacker, L., Hajdas, I., Kasper-Giebl, A., & Baltensperger, U. (2006). *Contributions of*
37 *fossil fuel, biomass-burning, and biogenic emissions to carbonaceous aerosols in Zurich as traced by 14 C*.
38 <https://doi.org/10.7892/boris.18245>
- 39 Trnka, M., R tter, R. P., Ruiz-Ramos, M., Kersebaum, K. C., Olesen, J. E.,  alud, Z., & Semenov, M. A. (2014). Adverse weather
40 conditions for European wheat production will become more frequent with climate change. *Nature Climate Change*, *4*(7), 637–
41 643. <https://doi.org/10.1038/nclimate2242>
- 42 Van der Voort, T. S., Mannu, U., Hagedorn, F., McIntyre, C., Walthert, L., Schleppei, P., Haghypour, N., & Eglinton, T. I. (2019). Dynamics
43 of deep soil carbon - Insights from 14C time series across a climatic gradient. *Biogeosciences*, *16*(16), 3233–3246.
44 <https://doi.org/10.5194/bg-16-3233-2019>
- 45 Vandenbroucke, M., & Largeau, C. (2007). Kerogen origin, evolution and structure. In *Organic Geochemistry* (Vol. 38, Issue 5, pp. 719–
46 833). <https://doi.org/10.1016/j.orggeochem.2007.01.001>
- 47 Voss, B. M., Peucker-Ehrenbrink, B., Eglinton, T. I., Spencer, R. G. M., Bulygina, E., Galy, V., Lamborg, C. H., Ganguli, P. M., Montlu on,
48 D. B., Marsh, S., Gillies, S. L., Fanslau, J., Epp, A., & Luymes, R. (2015). Seasonal hydrology drives rapid shifts in the flux and
49 composition of dissolved and particulate organic carbon and major and trace ions in the Fraser River, Canada. *Biogeosciences*,
50 *12*(19), 5597–5618. <https://doi.org/10.5194/bg-12-5597-2015>
- 51 Wacker, L., Fahrni, S. M., Hajdas, I., Molnar, M., Synal, H. A., Szidat, S., & Zhang, Y. L. (2013). A versatile gas interface for routine
52 radiocarbon analysis with a gas ion source. *Nuclear Instruments and Methods in Physics Research, Section B: Beam Interactions*
53 *with Materials and Atoms*, *294*, 315–319. <https://doi.org/10.1016/j.nimb.2012.02.009>
- 54 Xenopoulos, M. A., Downing, J. A., Kumar, M. D., Menden-Deuer, S., & Voss, M. (2017). Headwaters to oceans: Ecological and
55 biogeochemical contrasts across the aquatic continuum. In *Limnology and Oceanography* (Vol. 62, pp. S3–S14). Wiley Blackwell.
56 <https://doi.org/10.1002/lno.10721>
- 57 You, X., Li, X., Sillanp  , M., Wang, R., Wu, C., & Xu, Q. (2022). Export of Dissolved Organic Carbon from the Source Region of Yangtze
58 River in the Tibetan Plateau. *Sustainability (Switzerland)*, *14*(4). <https://doi.org/10.3390/su14042441>
- 59 Zobrist, J., & Reichert, P. (2006). Bayesian estimation of export coefficients from diffuse and point sources in Swiss watersheds. *Journal*
60 *of Hydrology*, *329*(1–2), 207–223. <https://doi.org/10.1016/j.jhydrol.2006.02.014>
- Zobrist, J., Schoenenberger, U., Figura, S., & Hug, S. J. (2018). Long-term trends in Swiss rivers sampled continuously over 39 years
reflect changes in geochemical processes and pollution. *Environmental Science and Pollution Research*, *25*(17), 16788–16809.
<https://doi.org/10.1007/s11356-018-1679-x>
- Zobrist, J., Sigg, L. M. C., Schoenenberger, Ursula, Sigg, L. M. C., & Sigg, L. M. C. (2004). *NADUF - thematische Auswertung der*
Messresultate 1974 bis 1998. Eidgen ssische Anstalt f r Wasserversorgung, Abwasserreinigung und Gew sserschutz, EAWAG.
- Zubler, E. M., Fischer, A. M., Liniger, M. A., Croci-Maspoli, M., Scherrer, S. C., & Appenzeller, C. (2014). Localized climate change
scenarios of mean temperature and precipitation over Switzerland. *Climatic Change*, *125*(2), 237–252.
<https://doi.org/10.1007/s10584-014-1144-x>